RED CELL MEMBRANE COMPONENTS DEPOSITED ON CONTACTING SURFACES

INVESTIGATION OF RED BLOOD CELL/FOREIGN SURFACE CONTACT: THE DEPOSITION OF MEMBRANE DERIVED MATERIAL

By

NORMA BORENSTEIN, B.ENG.

A Thesis

Submitted to the School of Graduate Studies

in Partial Fulfilment of the Requirements

for the Degree

Master of Engineering

McMaster University

(December) 1985

MASTER OF ENGINEERING (1985) MCMASTER UNIVERSITY

(Chemical Engineering) Hamilton, Ontario

TITLE: Investigation of Red Blood Cell/Foreign Surface Contact: The Deposition of Membrane Derived Components

AUTHOR: Norma Borenstein, B. Eng. (McGill University, Montreal)

SUPERVISOR: Professor J. L. Brash

NUMBER OF PAGES: xi, 92

ABSTRACT

An investigation of red blood cell interactions with contacting foreign surfaces is reported. The purpose of the study was to provide evidence to test the hypothesis that red cell membrane related deposit occurs when a suspension of red cells are exposed to a foreign surface. This membrane derived deposit is speculated to inhibit fibrinogen and albumin adsorption to glass and polyethylene (1,2).

Experiments consisted of flowing suspensions of washed human red cells through a column packed with spherical glass beads. The column is then washed to remove suspended cells and eluted using a mild detergent solution. The red cells were observed to have retained their biconcave shape after passage through the column. The eluates are examined by UV-visible spectroscopy and SDS-PAGE, and are found to contain cell membrane components. It is therefore concluded that membrane material had been deposited on the bead surface. The SDS-PAGE data show that membrane skeleton proteins are missing from the eluate, while SEM examination indicates the presence of filamentous deposits on the bead surfaces. These data suggest that cell-surface interactions may occur through a tether-type mechanism involving extrusion of part of the red cell membrane.

A 3 level, 3 factor fractional factorial design was used to quantitatively investigate the deposition in the column and to assess the effect of experimental variables on the phenomenon. The three factors studied were hematocrit, surface shear rate, and the presence

of plasma in the suspending medium. Statistical analysis of the data generated indicates a positive correlation between hematocrit and the amount of surface deposit. However no correlation for the effects of shear rate or plasma content could be established

In summary, red cell membrane components on contacting foreign surfaces were identified and a preliminary description of the phenomenon involved obtained. The deposit of membrane material is discussed in relation to Uniyal's "red cell effect" (1), and in the context of foreign surface induced thrombosis. It is hoped that this work will promote greater respect for the red cell as an important element in blood biomaterials interactions, and will prompt continued investigation on Uniyal's and other potential "red cell effects".

ACKNOWLEDGEMENTS

The author would like to thank those individuals without whose assistance this work could not have been accomplished.

Thanks are due to Dr. J. L. Brash for his supervision of this project. For their technical advice and stimulating discussions, the author would like to thank Jacqueline Thibodeau, Josephine Kush and Lorraine Skupny-Garnham.

She also wishes to acknowledge the moral support, and invaluable assistance from her husband, Neal Gordon, for the course of this work and especially for the preparation of this manuscript.

TABLE OF CONTENTS PAGE

Abstract iii

Acknowledgements v

List of Figures x

List of Tables xi

Chapter 1 Objectives and Introduction 1

Chapter 2 Literature Survey 5

2.1 Foreign Surface Induced Thrombosis 5

2.1.1 Coagulation Mechanisms 5

2.1.2 Platelets, Leukocytes and Red Cells 7

2.2 Red Blood Cells 10

2.2.1 Introduction 10

2.2.2 Red Cell Membrane; Lipid Globular Protein Model 13

2.2.3 Red Cell Membrane; Composition 15

a) Proteins 15

b) Lipids 17

2.2.4 Red Cell Shape and Deformability 21

a) Role of Membrane Skeleton 21

b) Lipid Losses and Cell Shape Changes 21

c) Biophysical Behaviour of Cell Membrane 23

Chapter 3 Methods and Procedures 27

3.1 Red Cell Suspensions 27

3.2 Ghost Cell Preparation 28

3.3 Hemoglobin Assay 28

3.4 ^{99m}Tc Labelling of Red Cells 30

3.5 Sodium Dodecyl Sulfate - Polyacrylamide Gel Electrophoresis (SDS-PAGE) 31

3.6 Ultraviolet-Visible Spectroscopy 32

3.6.1 Principles 32

3.6.2 Area Under Chromatograms 35

3.7 Packed Columns 36

3.7.1 Glass Bead Preparation 36

3.7.2 Column Dimensions and Packing Material 36

3.7.3 Surface Area 37

3.8 Experimental Protocol for Red Cell/Packed Column Experiments 37

3.9 Experimental Design 41

Chapter 4 Results and Discussion 45

4.1 Packed Column: Preliminary Experiments to Establish Experimental Protocol 45

4.1.1 Packing Material: Selecting Beads Size 45

4.1.2 Flow Rate and Shear Rate in Column 46

a) Power Law Rheological Model for RBC's 46

b) Column Conditions 48

c) Verification of Red Cell "Biostability" 50

4.2 Qualitative Analysis of Column Eluates (Red Cell Membrane Material) 51

4.2.1 UV-Visible Spectroscopy 51

4.2.2 SDS-PAGE: Identification and Proposed Modes of Deposition of Red Cell Membrane Material 54

4.2.3 Scanning Electron Microscopy 59

4.2.4 Effect of Divalent Cations on Deposition of Membrane Material 63

4.3 Quantitative Analysis 64

4.3.1 ^{99m}Tc Labelled Red Cells; Experiments 64

4.3.2 3^3 Fractional Factorial Design 67

Chapter 5 Summary and Conclusions 76

References 79

Appendix A (i) Red Cell Suspensions 83

(ii) Phosphate Buffered Saline 83

Appendix B Hemoglobin Assay Modification 84

Appendix C Gel Electrophoresis Information

(i) SDS-PAGE Buffers and Reagents 85

(ii) Silver Stain 86

Appendix D A_{220} Miscellaneous Information

(i) Variance for Absorbance at 220 nm 88

(ii) Standard Deviation of Calculated y Values 88

Appendix E $\dot{\gamma}_s$ Trial and Error Calculations 89

Appendix F Experimental Design Raw Data 91

LIST OF FIGURES PAGE

2.1 Coagulation Cascade 6

2.2 Coagulation Cascade: Feedback Loops 8

2.3 Stages of Thrombus Formation on Foreign Surfaces 11

2.4 Red Blood Cell Shape and Dimensions 12

2.5 Lipid Globular Protein Model for Red Cell Membrane 14

2.6 SDS-PAGE; Schematic of a Gel 16

2.7 Red Cell Membrane; Organization of the Cytoskeleton 18

2.8 Asymmetric Phospholipid Distribution for Human Red Cell Membrane 20

2.9 SEM of Red Cell Tethers 25

3.1 Standard Curve for Hemoglobin Assay 29

3.2 SDS-PAGE System; Principles of Operation 33

3.3 UV-Visible Spectrum of Solubilized Ghost Cells 34

3.4 Column Configuration 38

4.1 UV-Visible Spectra of Various Samples 52

4.2 SDS-PAGE of Various Samples 55

4.3 Estimate of Membrane Pore Size vs. Membrane Tension 58

4.4a-d SEM of Glass Beads for PBS Experiments 60

4.5a-b SEM of Glass Beads for Plasma Experiments 62

4.6 Schematic of 11% Gel; Autoradiograph (^{99m}Tc) 66

4.7a-c Graphical Representation of Experimental Design Data 71

LIST OF TABLES PAGE

3.1	Hematocrit Recipes	27
3.2	^{99m}Tc Red Cell Labelling Protocol	31
3.3	Experimental Design Matrix	42
3.4	Scaling Equations	42
4.1	Increase in Hemoglobin Content of Supernatant After Passage Through Column	45
4.2	Linear Regression Results For Power Law Parameter Based on Data from Brooks et al (58)	47
4.3	Interpolated n and k values	48
4.4	Liquid Head Corresponding to Various Shear Rates	50
4.5	Comparison of Column Elution Profiles With and Without Glucose in Suspending Medium	51
4.6	EDTA/EGTA Experiment Results	63
4.7	^{99m}Tc Experiment Results, Deposition of Radioactivity on Glass Beads Under Various Conditions	65
4.8	Experimental Design Results	68
4.9a	F-Test Summary: y_{A220} Data	70
4.9b	F-Test Summary: y_{A280} Data	70

OBJECTIVES AND INTRODUCTION

Currently progress in the field of biomaterials is indicated not so much by the availability of truly biocompatible artificial materials, but by the growing body of knowledge concerning "bio-incompatibility" of non-physiological surfaces; i.e. concerning the interactions of available biomaterials with the physiological environment. In the area of blood-compatible biomaterials the prospects for a truly and completely compatible replacement material seem remote, and drug therapy using anticoagulants is always required concurrently with available implant materials. This should not imply a lack of success in the development of physiologically tolerable materials. Materials such as segmented polyurethanes (e.g. Biomer^{R}), hydrogels, and heparinized polymers have been used in conjunction with drug treatments in extracorporeal blood contacting devices (heart-lung machines) and as biomaterials for implants (Jarvik VII artificial heart)(3). Some more recent innovations include plasma polymerized silicone coatings (4) or the use of electrical polarization to inhibit thrombus formation (5). However, ultimately the key lies in gaining a better and more complete understanding of the "bio-incompatible" blood/surface situation. The most crucial complications of blood contacting a foreign surface are thrombosis, involving blood coagulation and platelet activation, and potentially the most serious downstream consequence, thromboembolism.

When blood is exposed to a foreign surface, the surface develops within seconds a film of approximately 50 Å composed essentially of protein, most likely fibrinogen (6). This protein film dramatically changes the substrate with regard to surface charge, texture and chemistry (6). In approximately one minute the adsorption proceeds not to an equilibrium but to a critical thickness, usually 200 Å, sufficient for platelet attraction and adhesion (6). Extensive research has been and is being conducted regarding protein adsorption (isotherms, kinetics) of the individual plasma proteins (7,8). Also the role of platelets in coagulation and thrombosis on foreign surfaces has been extensively studied. Briefly, platelets arrive at the surface and begin a self propagating sequence of adhesion, release and aggregation, which contributes to thrombus growth.

It is generally assumed that intact red cells will have little if any direct effect on the blood-foreign surface interactions (9), but the potential of red cells to influence platelet behaviour by physical (hemodynamics) or biochemical (ADP release) means has been inferred (10,11). A recent report by Vroman et al (12) on plasma protein adsorption and platelet adhesion in narrow spaces of "clot-promoting surfaces" indicates primarily that platelets adhere only where fibrinogen remains adsorbed, but also notes that "whole blood leaves a ring of platelets corresponding to that of fibrinogen; in absence of erythrocytes the ring of platelets deposited is smaller" (12). Several publications have hypothesized that red cells contact the foreign surface and subsequently "deposit" material that

influences plasma protein adsorption (1,2), or platelet adhesion (13), and general inferences have been made regarding the potential role of this cellular deposit in artificial surface biocompatability, both in in vitro (14) and ex vivo (15) studies. To be more specific, Uniyal and Brash (1) provided evidence, by means of hemolysate versus red cell ghost experiments, which implies that the source of the "red cell effect" (i.e. the inhibition of plasma protein adsorption by red cells) is the cell membrane.

In sum, it may be that the role of red blood cells in the adverse response of blood to foreign surfaces, has been largely overlooked. The purpose of this present study was therefore to investigate the interactions of human red blood cells with a contacting foreign surface. The specific objectives were:

a) to establish an acceptable protocol to study red cell-surface contact using a packed column for large surface area exposure; i.e. a protocol which maintains biological stability of cells for duration of experiment.

b) to develop methods for qualitative identification and quantitative determination of material deposited on the foreign surface arising from the red cell.

c) to evaluate the effect, if any, of hematocrit, presence of plasma proteins, and shear rate on the amount of material deposited.

d) to re-evaluate the potential role of red cells in the overall scheme relating to biocompatibility of foreign materials.

It was hoped that the results of this investigation will contribute uniquely to the growing body of knowledge concerning blood/surface interactions, and in particular shed light on the "red cell effect" described by Uniyal and Brash (1); i.e. that protein

adsorption, the primary reaction in blood-surface contact, is inhibited in the presence of red blood cells.

LITERATURE SURVEY

2.1 Foreign Surface Induced Thrombosis

2.1.1 Coagulation Mechanisms

Foreign materials in contact with blood either extracorporeally or as vascular implants, trigger the mechanism of blood coagulation contributing to thrombosis, often followed by the formation of thromboemboli. It should be noted that damage to normal blood vessels can initiate these same responses. The coagulation process is best described as a cascade of enzymatic reactions leading to the formation of fibrin. Coagulation is initiated either by the activation of a glycoprotein, Factor XII (Hageman factor) or release of a tissue factor (thromboplastin). The former gives rise to a reaction sequence referred to as the "intrinsic" system, the latter initiates the "extrinsic" system. Figure 2.1 (16) illustrates the cascade pathways and the factors involved.

In general the intrinsic system is considered to be the predominant pathway involved in blood-foreign surface interactions, due to the fact that Hageman factor (Factor XII) is readily activated by surface contact (16). However, due to the complexity of the coagulation mechanisms it is a gross oversimplification to consider the extrinsic and intrinsic systems as independent. Aside from the common end sequence of reactions (see Figure 2.1), the two systems influence and reinforce each other via feed back loops and cross-over

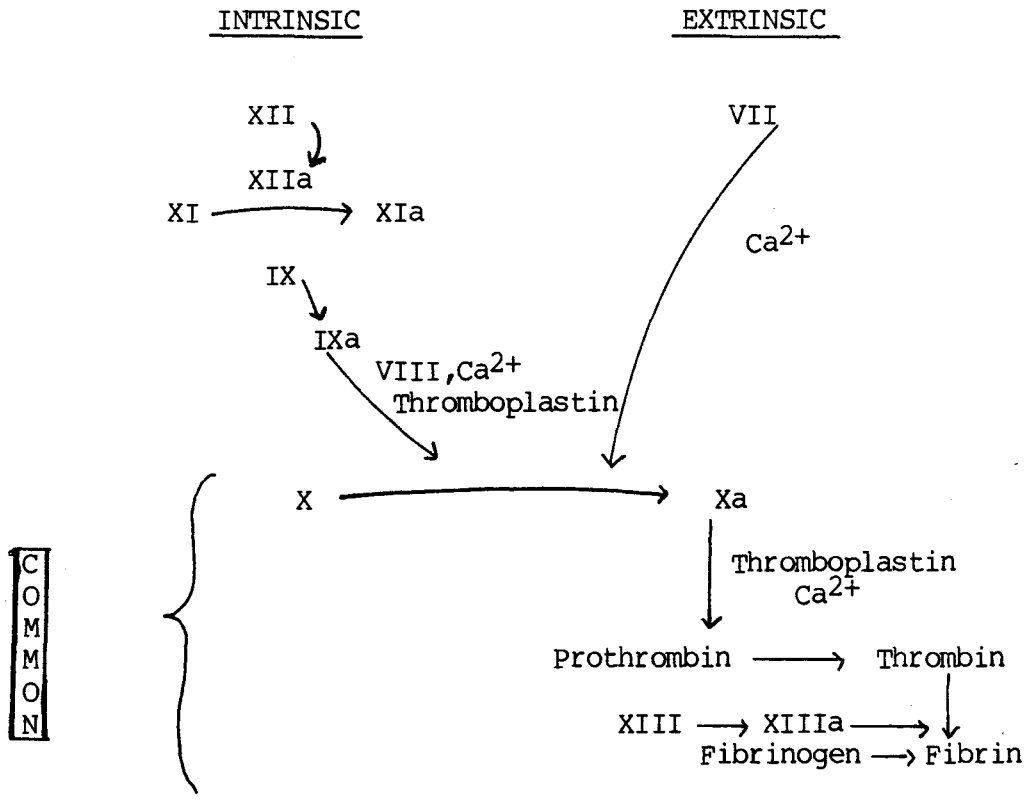

Figure 2.1 Coagulation Cascade (16)

activations. In particular Factor Xa and thrombin formed from either pathway, feed back to activate Factors VIII and V, and the Factor Xa loop can increase or inhibit its own activation by Factor VIIa. The earlier, separate phases of the two pathways, are linked such that Factors IXa, XIIa, XIa and kallikrein activate Factor VII and Factor IX can be directly activated by Factor VIIa. To add to the complexity, the activation of Factor XI can occur through a platelet/collagen related reaction, without involving Factor XII (8,16,17). These feed back type relationships are illustrated in Figure 2.2.

The coagulation system can be inhibited (if not prevented) by the use of anticoagulants. The simplest intervention is accomplished by the use of chelating agents such as citrate or ethylenediaminetetra acetic acid (EDTA) to "immobilize" calcium ions which are required in several of the cascade reactions (see Figure 2.1). Anticoagulants such as either heparin or coumarin derivatives prevent the activation of various clotting factors. Specifically, heparin catalyzes the antithrombin (natural anticoagulant for hemostasis) inactivation of Factors XIIa, XIa, IXa, Xa, and thrombin, whereas coumarin interferes with vitamin K effects on Factors II (prothrombin), VII, IX, and X. Vitamin K allows for an increased calcium affinity, hence facilitating the binding of factors to platelet phospholipid (16).

2.1.2 Platelets, Leukocytes and Red Cells

Of the formed elements of blood, platelets have received the

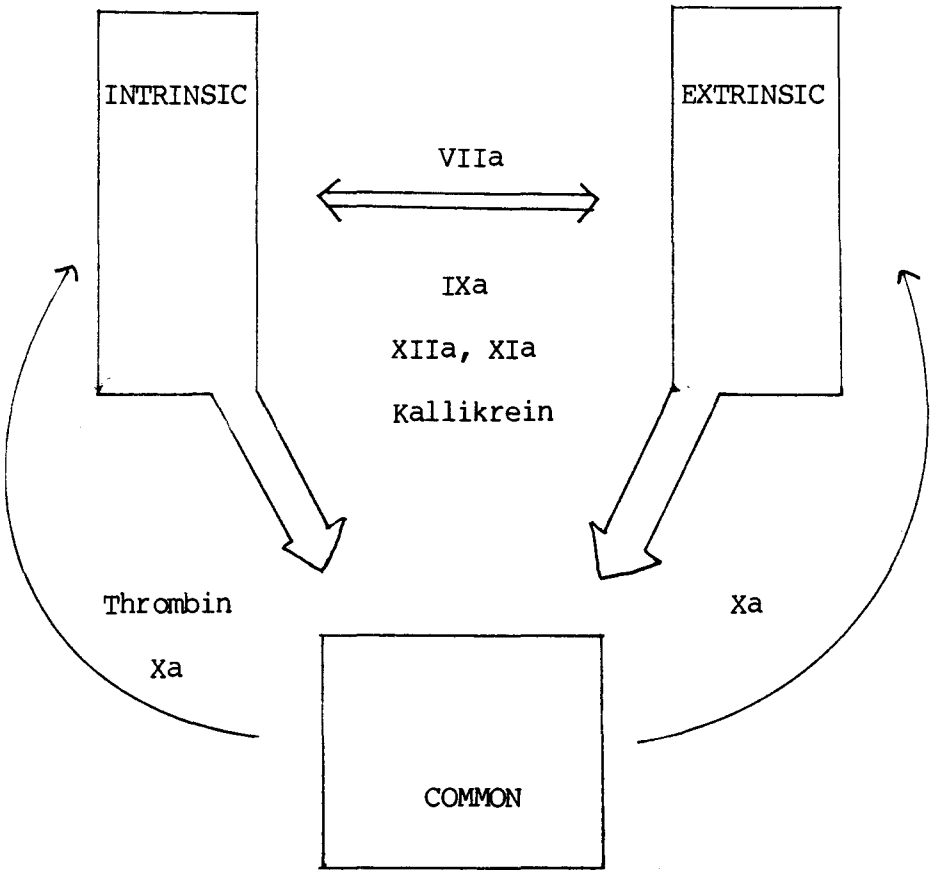

Figure 2.2 Coagulation Cascade Feedback Loops (16)

most attention in the study of blood-surface interactions. Their role in thrombus formation is to adhere on the surface followed by the release of adenosine diphosphate (ADP) and thromboxane A_2 (TxA_2) (16). Both ADP and TxA_2 stimulate platelet aggregation, thus creating a self-propagating platelet plug at the blood-material interface. Phospholipid exposed as a result of platelet aggregation facilitates the activation of both Factor X and prothrombin. In addition, many coagulation factors are attached to, and most activation steps occur on, the platelet membrane phospholipid surface.

The role of leukocytes in blood-material interactions can be related to their ability to recognize the surface as foreign, after protein adsorption and platelet adherence have occurred (17). They are not generally considered to have a direct role in thrombus formation.

The role of intact red cells is generally assumed to be minimal, and to be limited to hemodynamic effects in terms of promoting diffusion of platelets to the thrombus or potentially thrombotic site. However, it seems that the potential of red blood cell involvement may have been overlooked. Intracellular components, particularly ADP, released from damaged or lysed red cells could stimulate platelet aggregation on foreign surfaces. This has not however been proven. This study concentrates on intact red cells contacting surfaces, therefore leaky or damaged red cell effects are not an issue. Directly involved in thrombus formation, red cells are most noted when trapped in the fibrin mesh, creating the "red

thrombus". However it is important to consider the effect of red cells on other blood elements. It has been shown that red cells inhibit plasma protein adsorption and increase platelet adhesiveness to foreign surfaces (1,2). Furthermore it has been suggested that the cell membrane is the source of the phenomenon (1). One might speculate that the red cell role in foreign surface induced thrombosis could involve a) interfering with plasma protein adsorption, and b) affecting platelet adhesion and aggregation, and c) depositing membrane components which expose a phospholipid surface, an activation site for coagulation factors. This last point may prove to be the most interesting in light of recent reports that red cell membrane proteins are immunologically and perhaps functionally related to platelet membrane proteins (18).

To complete this section, a brief schematic of thrombus formation on foreign surfaces is shown in Figure 2.3. The formation of either a "red" (predominantly trapped red cells) or "white" (predominantly platelets) thrombus is dependent on the flow regime, the former occurring at low and the latter at high shear rates.

2.2 Red Blood Cells

2.2.1 Introduction

The erythrocyte is defined as "a red blood cell or corpuscle; it is one of the formed elements of blood. Normally, in the human, the mature form is a non nucleated, yellowish, biconcave disc, containing hemoglobin and transporting oxygen" (20).

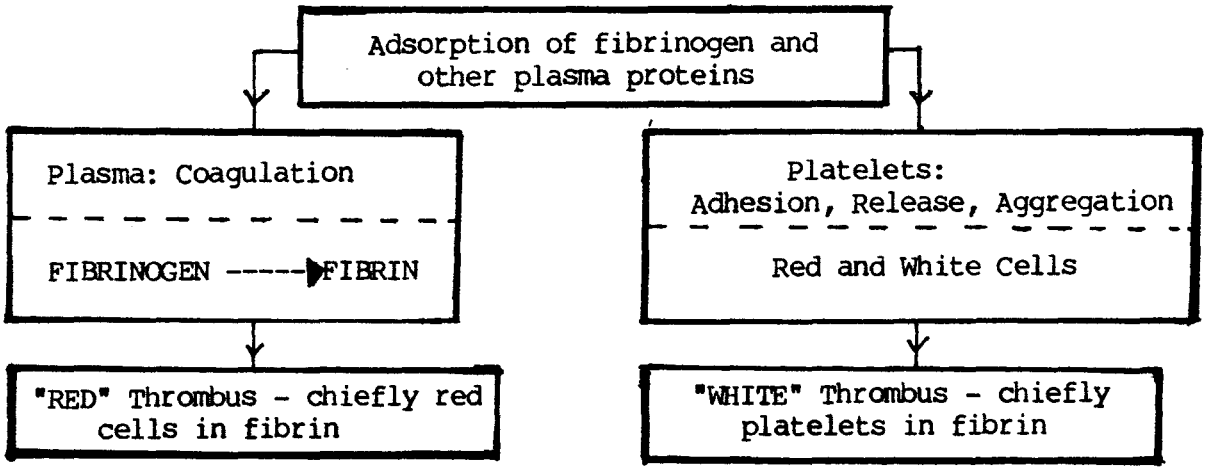

Figure 2.3 Stages of Thrombus Formation on Foreign Surfaces (19)

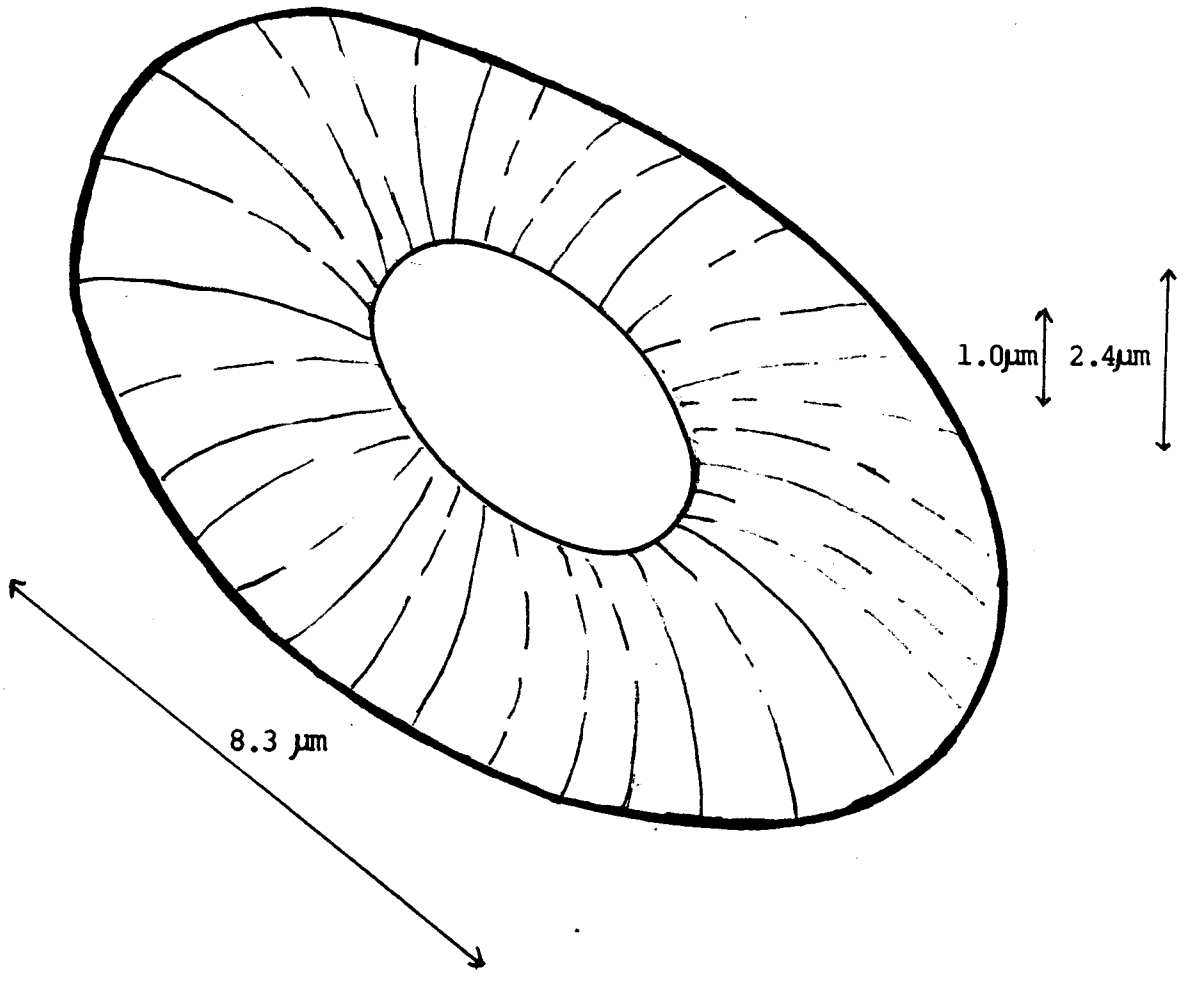

Figure 2.4 Red Blood Cell Shape and Dimensions

When the red cell enters the circulation, after proliferation and hemoglobinization within the bone marrow, it is no longer nucleated and exists primarily to transport the respiratory gases. The normal biconcave/discoid shape, illustrated in Figure 2.4, of the red cell exposes 25-30% greater surface area than would a sphere having the same volume, a significant and obvious advantage for gas exchange.

Typical red cell dimensions are: diameter 8.3 μm (long axis), surface area 140 μm^2, and volume 90 μm^3. The red cell membrane structure and composition govern most cell/surface interactions and contact phenomena.

2.2.2 Red Cell Membrane; Lipid Globular Protein Model LGPM[a] (9)

The lipid globular protein mosaic model (Figure 2.5), builds on the central theme of earlier models, namely that there is a lipid bilayer within the membrane. The LGPM model proposes that globular proteins are incorporated to varying degrees into the phospholipid bilayer and are distributed randomly in the plane of the membrane. The terms "integral" and "peripheral" were introduced by Singer (21) to describe protein associated with the membrane lipid bilayer. Literally, integral proteins by virtue of their amphipathic nature are integrated into the bilayer structure, with the hydrophilic regions

a. Singer and Nicolson used the term "fluid mosaic model" (21).

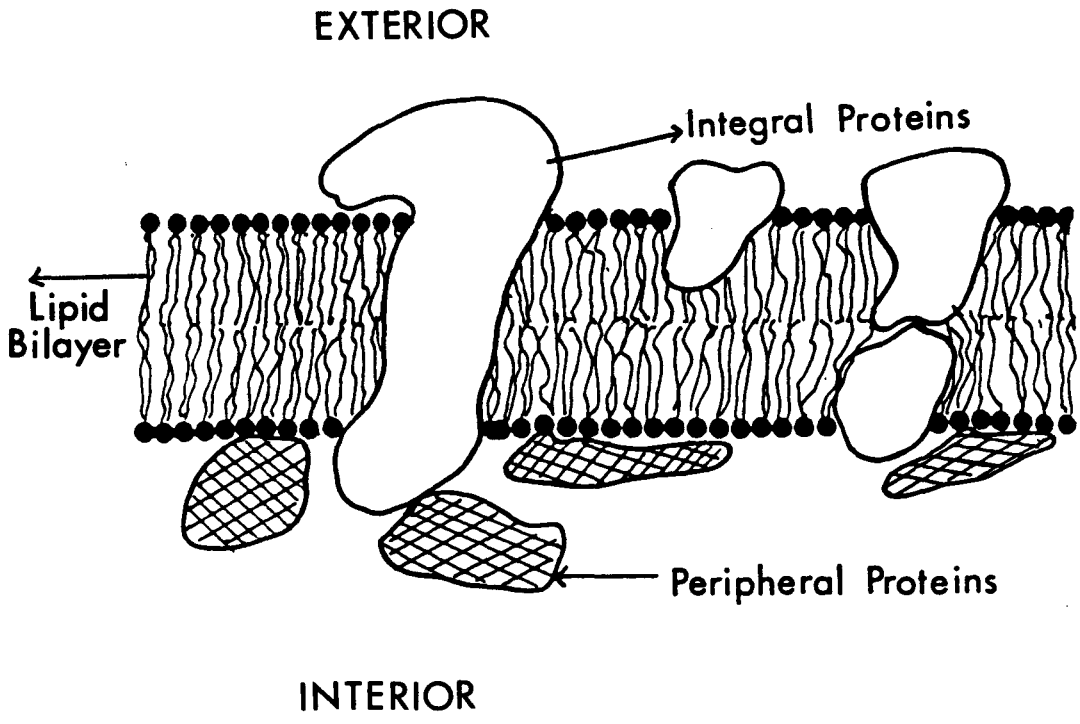

Figure 2.5 Lipid Globular Protein Model For Red Cell Membrane(9)

near the membrane surface (extra or intra cellular) and the hydrophobic regions imbedded in the lipid layers. The peripheral proteins are associated with the membrane surfaces and are not likely to be incorporated into the lipid matrix of the membrane. The description "fluid mosaic model" as used by Singer and Nicolson (21) emphasizes that phospholipids as portrayed in the LGPM could be fluid under physiological conditions. Examples of both peripheral and integral proteins have been isolated from red cell ghosts (9).

2.2.3 Red Cell Membrane; Composition

a) Proteins

Approximately half the red cell membrane mass is accounted for by lipids (primarily phospholipid and cholesterol) and glycolipids, and half by protein and glycoprotein (22). The basic protein composition of the red cell membrane can be determined using one-dimensional sodium dodecyl sulfate (SDS) polyacrylamide gel electrophoresis (PAGE), to differentiate the proteins by molecular weight. A schematic of such a gel is shown in Figure 2.6. Proteins visualized by Coomassie Blue staining are numbered according to the scheme of Fairbanks et al (23). Periodic acid Schiff (PAS) staining is used to detect another important group of red cell membrane proteins, the sialoglycoproteins (Figure 2.6 - nomenclature of Steck et al (24)) One dimensional SDS-PAGE gives a compact view of membrane composition. Considerably better resolution can be achieved with two-dimensional electrophoresis, for example isoelectric focusing in

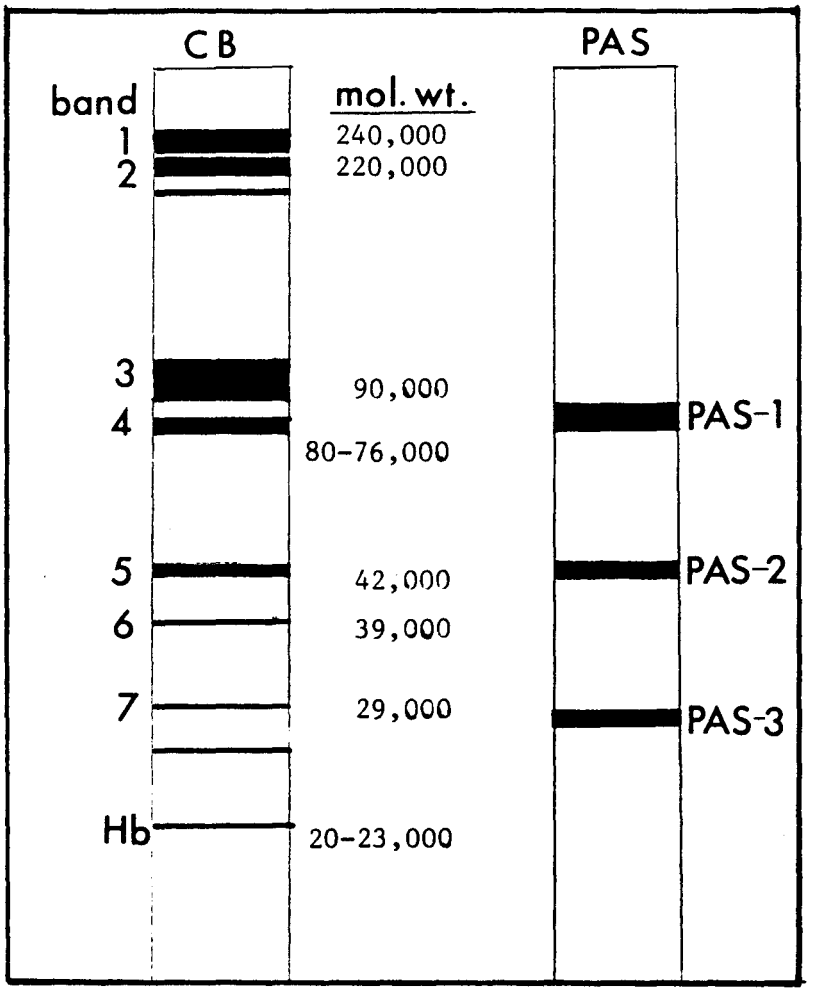

Figure 2.6 SDS-PAGE; schematic of a 5% gel, key to lanes: CB=Coomassie Blue, PAS=periodic acid Schiff; Additional nomenclature - bands 1,2 = spectrin, 3 = anion transport protein, 5 = actin, 6 = glyceraldehyde-3-phosphate dehydrogenase, PAS2 = "glycoconnectin" (22)

the first dimension and SDS-PAGE in the second (25). With this approach more than 90 polypeptides have been identified (26).

The proteins responsible for the characteristic red cell shape and for many of its mechanical properties form what is known as the membrane skeleton. This highly interconnected network of proteins, all of which are bound to the membrane, lies within 10 nm of the cell membrane. Triton X-100, a non-ionic detergent, solubilizes nearly all the membrane lipids and integral membrane proteins (22). The residue, "Triton Shell" is the most widely studied preparation of the red cell membrane skeleton. Following the nomenclature of Fairbanks (23) and Steck (24), the organization of the red cell membrane skeleton structure is illustrated in Figure 2.7 (27). The following quotation from a recent review on red cell membrane skeleton structure and function (28), illustrates the multifaceted role of the skeleton: "membrane skeleton confers stability on the lipid bilayer, is responsible for plastic deformation, regulates topography of surface receptors via attachment of their cytoplasmic segments and probably also plays an important role in transmembrane signaling".

b) Lipids

The lipid bilayer structure, is the "backbone" of the red cell membrane geometry. The four major classes of phospholipids identified in the bilayer are: phosphatidylcholine (PC), phosphatidyl ethanolamine (PE), phosphatidylserine (PS) and sphingomyeline (SM). In addition the membrane contains cholesterol (1:1 molar ratio to

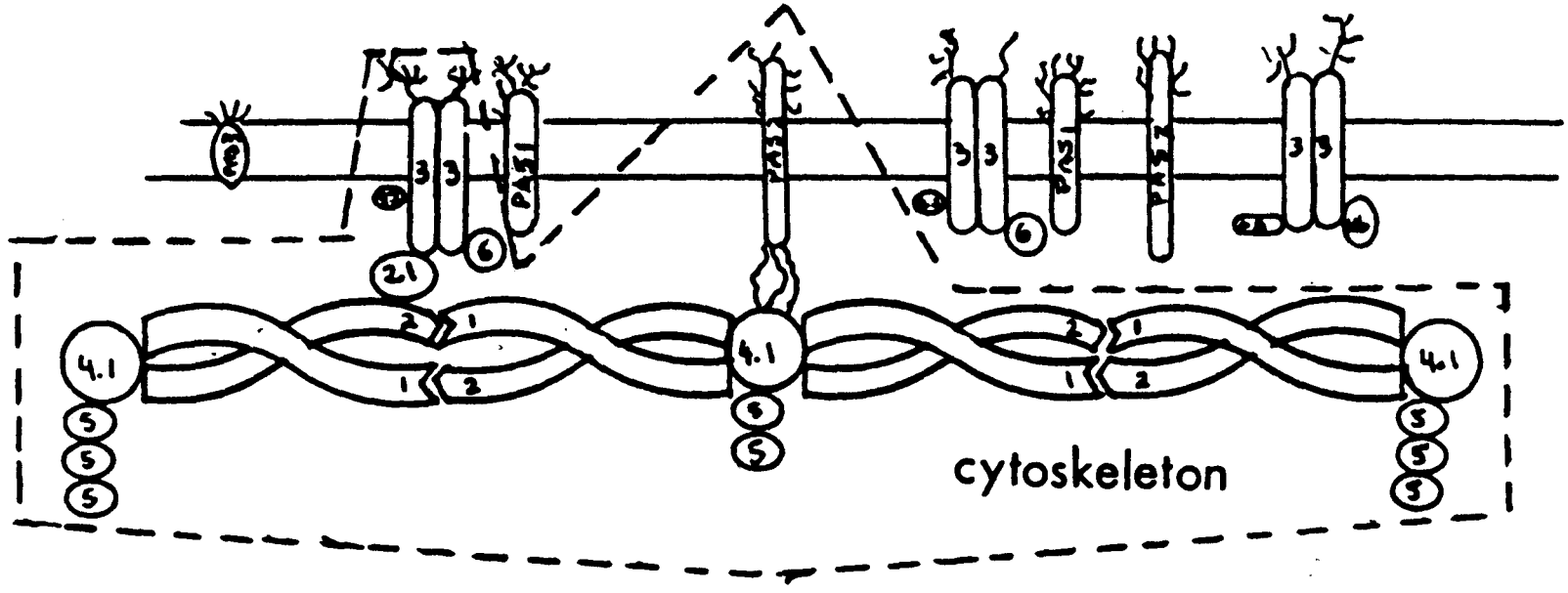

Figure 2.7 Red Cell Membrane; organization of the cytoskeleton (27)

Nomenclature as described in Figure 2.6 (see page 16)

phospholipid (29)), glycolipids, neutral lipids, and the intercalated proteins previously described. A general feature of the red cell membrane is that the lipid components are distributed asymmetrically across the thickness dimension, with the possible exception of cholesterol (29). The outermost lipid layer of a mature red cell membrane consists predominantly of choline-containing phospholipids, PC and SM, while the cytoplasmic or inner leaflet contains primarily aminophospholipids, i.e. PE and PS. The distribution of PC, SM, PE and PS in the membrane layers is represented by the bar diagram in Figure 2.8 (30). Maintenance of the specific asymmetric distribution of phospholipids in the bilayer, in particular the confinement of PS to the cytoplasmic surface, is an important role of the membrane skeleton. Acidic phospholipids, such as PS, if exposed extra-cellularly would have the potential to promote coagulation, with pathological consequences. An example showing the consequences of disturbing the phospholipid distribution is sickle cell anemia, where it has been shown that deoxygenated, irreversibly sickled red blood cells have increased PS and PE in the lipid matrix outer leaflet. As a result, blood containing sickled cells has decreased clotting time in vitro (31). This example highlights the potential for red cell membrane, perhaps modified by blood-material contact, to participate in coagulation and thrombus formation at the blood-material interface.

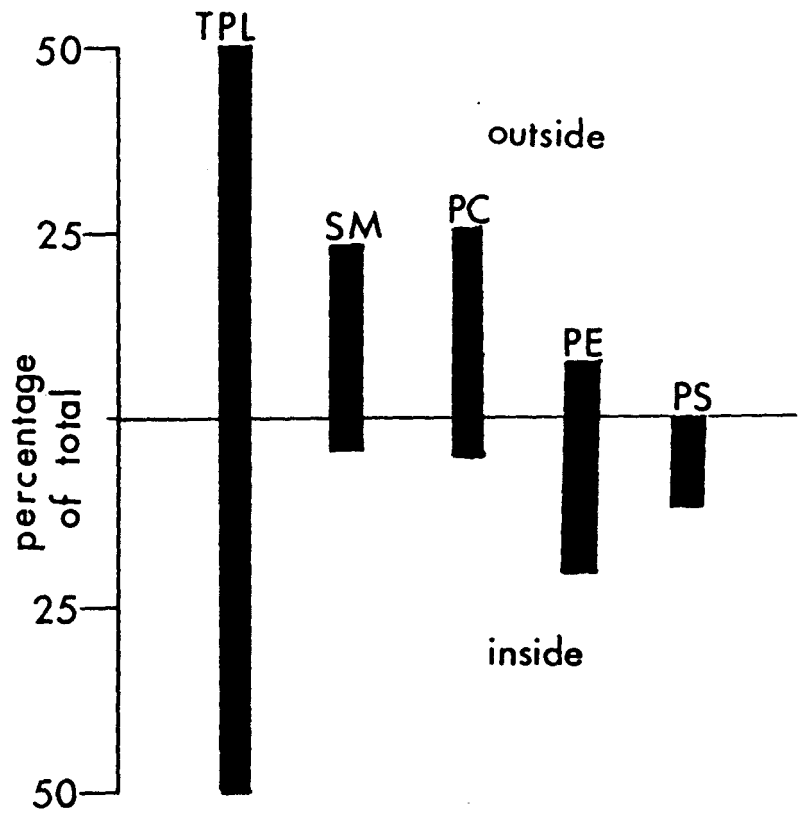

Figure 2.8 Asymmetric Phospholipid Distribution for Human Red Blood Cell Membrane (30)
TPL = total phospholipid
SM = sphingomyeline
PC = phosphatidylcholine
PE = phosphatidylethanolamine
PS = phosphatidylserine

2.2.4 Red Cell Shape and Deformability

a) Role of Membrane Skeleton

It has become increasingly clear that the membrane skeletal proteins are the key participants in the maintenance of the two unique features of the mammalian red blood cell, namely its biconcave disc shape and its remarkable deformability (32). Evidence in support of this hypothesis includes: 1) extraction of skeletal proteins, in particular spectrin and actin, from ghosts, initiates membrane fragmentation and extreme vesiculation (22), 2) "Triton shells" retain the shape of the parent ghost regardless of its nature; i.e. normal (biconcave), sickled or elliptical (22), and 3) skeletal protein deficiencies have been associated with abnormal red cell shapes found in several hereditary red cell disorders (22). Furthermore, the cytoskeletal structural organization influences the mobility and positioning of integral membrane proteins and lipids by direct or indirect associations with the cytoplasmic domains of these components (22). Some of the red cell characteristics, such as the typical discoid shape (32), are likely to be attributable to the combined properties of the cytoskeleton and lipid matrix. Without integral proteins or the cytoskeleton a membrane composed simply of lipid could not withstand the forces encountered in the circulation, and would be unstable even under static conditions (33).

b) Lipid Losses and Cell Shape Changes

The most obvious advantage of the red cell's biconcave disc

shape, is an increase in surface area for gas exchange, some 25-30% greater than that of a sphere (34). However, a more important benefit of the biconcave geometry is that it allows the red cell to undergo marked deformation while maintaining a constant surface area (32,35). The normal dimensions of the red cell can be extended linearly by more than 200%, yet an increase of only 2 to 4% in surface area results in cell lysis (36). Cells that have become spherical, for example due to a decrease in the osmolarity of the surrounding medium or through membrane fragmentation (from skeletal protein defects), are considerably less deformable and hence less viable in the circulation. Lipid losses are generally associated with red cell sphering.

Lipid loss from red cell membrane occurs naturally as a part of the ageing process (9). Consequently, the cell becomes less deformable and it is subsequently removed from the circulation. Two unnatural causes of lipid loss are: 1) increased intracellular calcium levels and 2) red cell contact with artificial materials (29,37).

Normally intracellular levels of calcium are extremely low, in the order of 10^{-2} mM compared to a plasma concentration of 2 mM (9). The low intracellular concentration is maintained by membrane permeability resistance to cations, and by an active calcium pump (energy source provided generally by ATP) (9). Increased levels of Ca^{2+} cause a marked decrease in the red cell membrane deformability. Mohandas et al (38) identified dehydration and an increase in internal

viscosity as the dominant mechanism of deformability loss, in contrast with previous hypotheses attributing the loss to increased membrane rigidity (38). The findings of Allan et al (39,40) indicate membrane losses in the form of "budding-off" of micro and nano vesicles (without substantial hemolysis) for calcium loaded red cells. Of particular interest is that the lipid to protein weight ratio of these vesicles was found to be approximately 2.8, some 4 times greater than in red cell membrane ghosts.

Contacting of cells with a foreign surface may produce dramatic effects on red cells such as immediate cell damage and lysis. Less "severe" contact conditions can result in a "premature ageing",i.e. lipid losses (7,37), of red cells. It has been reported, that red cells exposed to mechanical trauma (pumped in tubing) exhibit selective lipid and phospholipid losses prior to cell hemolysis (37). As shown by Keller and Yum (14), and hypothesized by Uniyal and Brash (1), red cells can contact the surface and potentially deposit membrane material without immediate red cell damage. Ex-vivo studies by Winters et al (15) also suggest red cell deposits on foreign materials. Recently the classical red cell tether "deposit" (see following section) has also been associated with lipid segregation from the red cell membrane (41).

c) Biophysical Behaviour of Cell Membrane

The red cell membrane is capable of exhibiting three types of "flow", depending on the magnitude and duration of the applied shear

stress (35,42,43). At low values of applied force (up to 10^{-6} dynes), for short time intervals (less than 100 seconds), the membrane exhibits viscoelastic solid behaviour; i.e. completely recoverable elastic extensions occur (32). For extended durations of the stress, "creep" typical of semi-solid responses is seen, implying that partly irreversible deformations exist (32). Larger forces (greater than 10^{-6} dynes) cause the membrane material to yield and flow, consequently, permanent "plastic" deformations occur. This third regime of viscoplastic flow is relevant to the study of red cell-surface interactions, as it gives rise to the formation of red cell "tethers" as shown in Figure 2.9. One of the first publications illustrating the tether phenomenon is the work of Hochmuth et al in 1972 (44). They reported on surface adhesion, deformation and detachment of red cells at low shear rates. The experiments involved allowing red cells to settle onto the surface (for various settling times), followed by determining the force required to detach the cells from the surface. The tethers, which resulted from the detaching red cells, appeared to be "clean breaks"; i.e. the red cell remains intact after the extraction of the tether, a "self-sealing" effect (44). In the report of Hochmuth et al, it was concluded that for low shear stresses at the surface (i.e. less than 8-10 dynes/cm^2), not only is cell/surface contact established but whole cell deposition and adhesion can occur. It was found that for "raw" glass the minimum critical stress required for cell detachment increased with increasing settling time from 10.5 dyne/cm^2 (at a settling time of 10 minutes) to

Figure 2.9 SEM of Red Cell Tethers (32)

15 dynes/cm^2 (settling time of 60 minutes). Cell adhesion forces were found to be significantly reduced for protein coated surfaces. Tether formation still occurred on the protein coated surface, although single point attachments resulting in one tether per cell rather than multiple tethers were observed (44).

The material characteristics of the membrane that determine whether or not viscoplastic flow occurs are: 1) the level of applied force above which the membrane material yields and begins irrecoverable flow, reported to range from 2 to 8 x 10^{-2} dyne/cm (36,42) and 2) the coefficient of surface viscosity (of the membrane) for plastic flow, approximately 10^{-2} dyne-s/cm (36,42). The critical shear stress required to produce tethering of a surface localized cell has been reported to be approximately 1.5 dyne/cm^2 (45). Obviously, variations in surface or flow conditions, fluid medium composition, hematocrit, etc., will have an influence on these values. This must be kept in mind when comparing results of different investigators.

METHODS AND PROCEDURES

3.1 Preparation of Red Cell Suspensions

Human blood drawn from healthy donors was collected in tubes containing acid citrate dextrose (ACD) anticoagulant (6:1, blood:ACD). The blood was centrifuged (1000 x g) twice for three minutes and the supernatant and buffy coat (white cells and platelets) were removed. The red cells were then washed three times in isotonic phosphate buffered saline (PBS) pH 7.35 with centrifugation (1000 x g, 10 minutes) between each wash. After washing the red blood cells were then resuspended in the desired medium; i.e. either PBS or autologous plasma, or 50% PBS/50% plasma, according to the proportions outlined in Table 3.1, to give the required hematocrit. The suspensions were used

Table 3.1 HEMATOCRIT RECIPES

% HCT	Volume of Packed Cells (ml)	Volume of Buffer (ml)
20	8	30
40	15	21
60	25	15

immediately after preparation. By this procedure the cells were washed and resuspended within 1 to 1.5 hours of the initial blood collection, thereby, overcoming the need to add glucose to the PBS

suspending medium to avoid ATP depletion. This was verified by running parallel experiments with PBS and PBS containing 1 g/l glucose.

3.2 Ghost Cell Preparation

Unsealed ghosts were prepared by Steck's method (46), incorporating the modifications of Burton et al (47). Washed cells were osmotically hemolyzed in ice cold 5mM sodium phosphate (0.5 ml packed cells:10 ml buffer), then centrifuged at 3000 x g for 15 minutes. After aspirating the supernatant, the two additional washes that followed were performed with 2.5 and 1.25 mM sodium phosphate, respectively.

3.3 Hemoglobin Assay

A colourimetric assay based on the cyanmethemoglobin method was used to determine the hemoglobin content of the red blood cell suspension supernatants. The principle of the assay is that in the presence of potassium ferricyanide (Drabkin's reagent) at alkaline pH, hemoglobin and its derivatives except sulfhemoglobin, are oxidized to methemoglobin. The methemoglobin reacts further with potassium cyanide to form cyanmethemoglobin which has a maximum absorbance at 540 nm. The colour intensity at this wavelength is proportional to total hemoglobin concentration (48). The protocol for using the Sigma reagents (48) was modified to determine the hemoglobin content of suspension supernatants, some 500 fold lower than that of whole blood (see Appendix B). Using a Beckman model 25 spectrophotometer, a

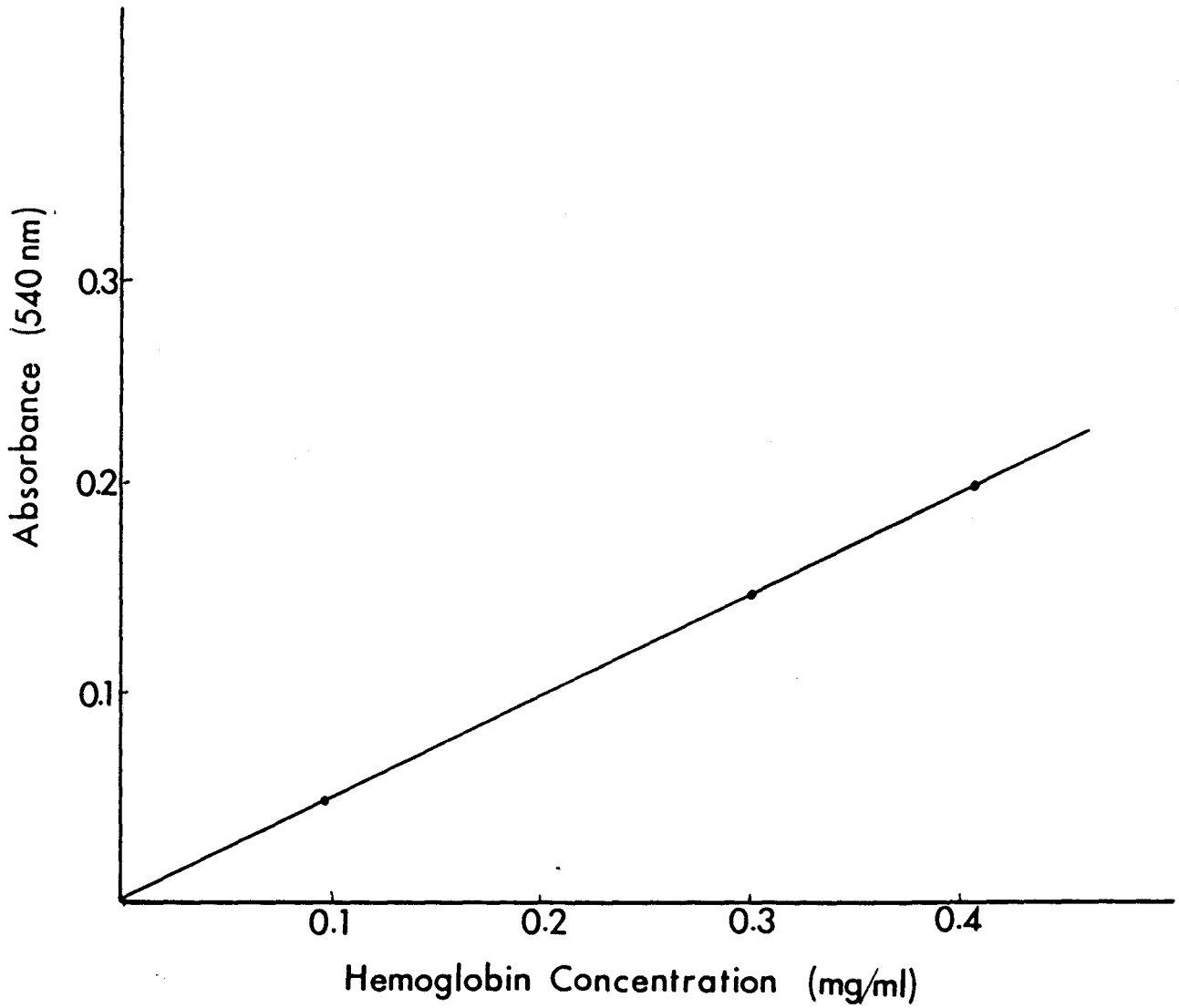

Figure 3.1 Standard Curve for Hemoglobin Assay

standard curve of A_{540} versus hemoglobin concentration was constructed with the Sigma reagents (Figure 3.1). The protocol used for the supernatant samples was as follows, 0.510 ml of the Drabkin's reagent (48) was mixed with 2 ml of sample. A_{540} readings were obtained and the hemoglobin concentration read from the standard curve shown in Figure 3.1.

3.4 ^{99m}Tc Labelling of Red Blood Cells

In an attempt to detect and quantify the material deposited on the column packing surface (see sections 3.7, 3.8 for description of packed column experiment used to expose surfaces to RBCs), red cells were labelled with ^{99m}Tc. It was assumed that the accumulation of radioactivity in the column would represent the amount of material deposited. ^{99m}Tc was chosen because it has been shown that part of the radioactive label is associated with the cell membrane as well as with hemoglobin (49). ^{51}Cr on the other hand has been shown to be associated uniquely with hemoglobin (49). Red cell labeling was achieved by a simple two step incubation procedure using stannous ions and sodium pyrophosphate solutions as a "linking" medium for the isotope. Table 3.2 outlines the labeling protocol. The isotope and labeling solutions were all obtained from McMaster University Radiopharmacy. After the bulk suspension was washed from the column, the beads were removed and placed into vials which were immediately counted using a Beckman Biogamma counter. The equation used to account for the six hour half-life decay is as follows;

$$N_o = N\exp(0.115524t) \qquad (3.1)$$

where N_o = counts at time 0
N = counts at time t
and t = time in hours.

Table 3.2 Tc99m Red Cell Labelling Protocol

Red Cell Suspension[a]	= R ml
Add "MIX"[b]	= 0.6 x R ml
Add heparin[c]	= 2 x R µl
Mix and Incubate	= 10 min
Add ^{99m}Tc	= 1-2 mCi
Mix and Incubate	= 10 min
Complete PBS washes	= 2 times

a unwashed RBC's resuspended in PBS to 40% Hct
b 1.9 ml sodium pyrophosphate (20mg/ml in 1N HCl) + 0.1 ml stannous chloride (20mg/ml in 1N HCl)
c Sigma heparin H-3125, 25,000 units in 10 ml PBS

3.5 Sodium Dodecyl Sulfate - Polyacrylamide Gel Electrophoresis (SDS-PAGE)

SDS-PAGE is used to separate and identify proteins based on molecular weight. The polyacrylamide gel acts as a stabilizing medium for the buffers, with pores small enough so that the matrix also provides a sieving effect. Proteins are separated according to charge density when a potential gradient is applied to the system. Solubilizing the proteins with the detergent SDS allows for separations based on molecular weight since the SDS binds to polypeptides with a constant weight ratio. The protein-detergent complex therefore has a constant charge per unit weight, and migrates through the polyacrylamide gel matrix towards the anode at a rate inversely related to the logarithm of the relative molecular mass.

Figure 3.2 illustrates the system involved. The buffers and gel recipes are listed in Appendix C(i), according to the Laemmli method (51). Protein visualization is achieved by staining the gel after electrophoresis. Conventionally, Coomassie Blue is used to stain the gel. However, for the samples eluted in the column experiments silver staining which is 10-50 fold more sensitive than Coomassie Blue (52) was used. Briefly, the gels are fixed in alcohol/acetic acid solutions and developed using the Biorad reagents. Reagent preparations and the silver stain protocol are given in Appendix C(ii).

3.6 Ultraviolet-Visible Spectroscopy

3.6.1 Introduction

Ultraviolet-visible spectroscopy is used to identify and quantify the material eluted from the columns. UV-visible spectra for solubilized membrane samples are quickly and easily obtained. Preliminary identification of the material eluted from the packed column surface can be accomplished by direct comparison to the spectrum obtained for solubilized red cell ghosts, illustrated in Figure 3.3. Typical absorbance maximum associated with protein is 280 nm and either 190 or 220 for lipids (53). Spectra for samples were run from 450 down to 190 nm as seen by example in Figure 3.3.

For determining quantitatively the amount of material deposited in the columns, the absorbance of eluate fractions are read at 220 and 280 nm, the latter as support data, and chromatograms created. The area under the curve is used as a measure of material deposited.

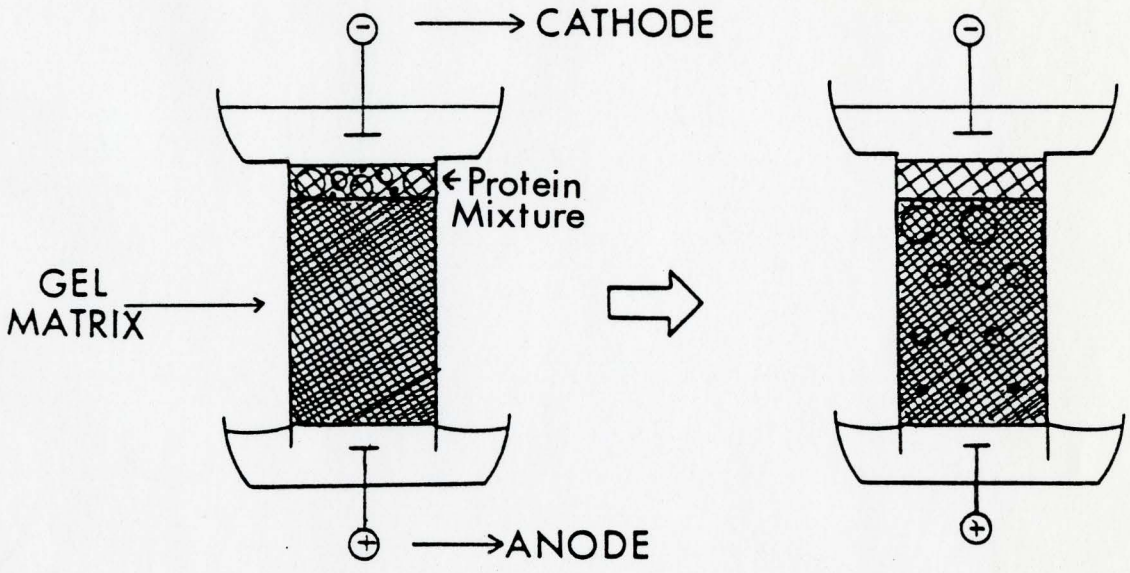

Figure 3.2 SDS-PAGE System; principle of operation

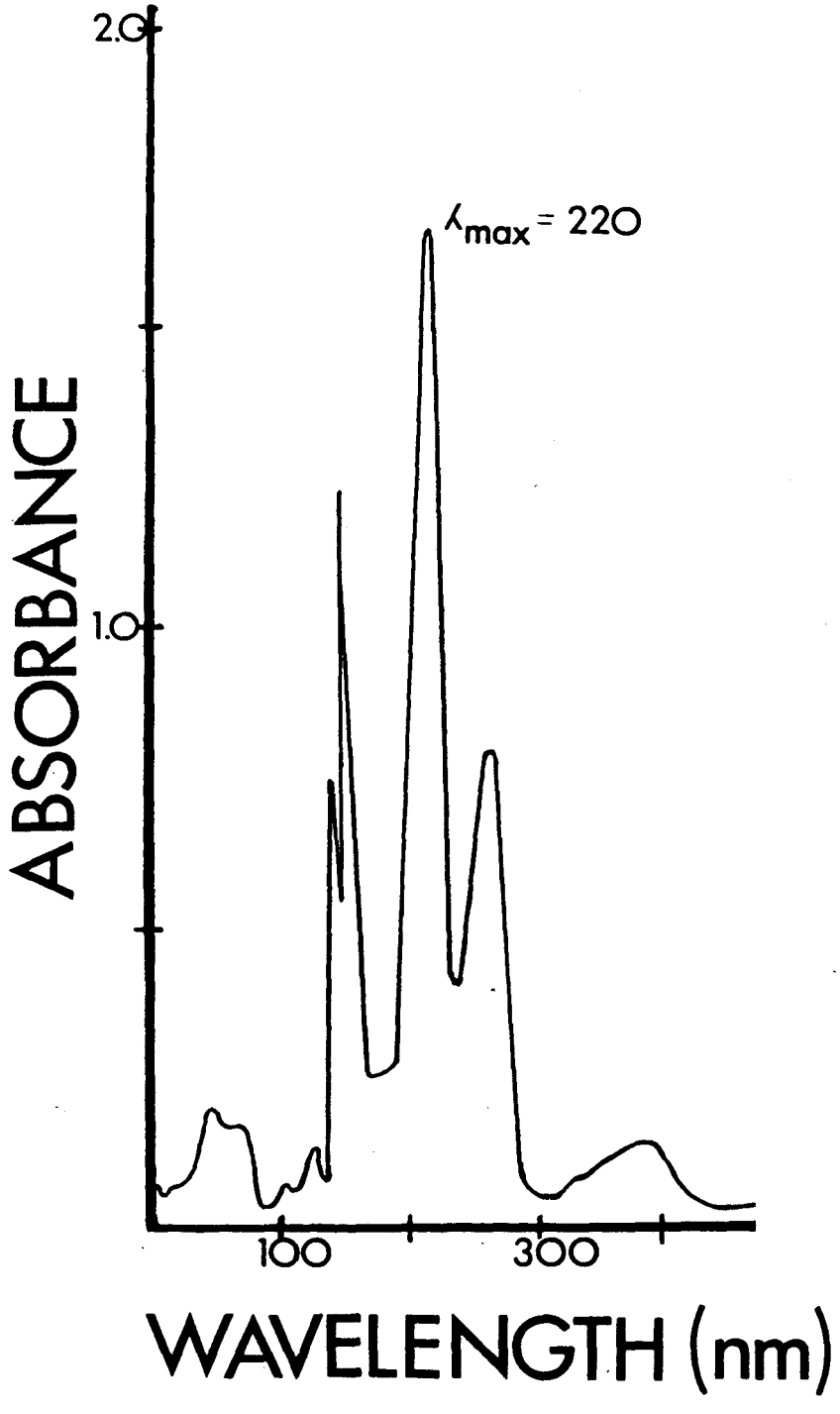

Figure 3.3 UV-Visible Spectrum of Solubilzed Ghost Cells

3.6.2 Area Under Chromatograms

The area under the absorbance versus eluted fraction chromatogram is calculated by numerical integration, using Simpson's rule:

$$A \quad h/3(y_0 + 4y_1 + 2y_2 + \ldots + 2y_{n-2} + 4y_{n-1} + y_n) \qquad (3.2)$$

where A = area under the curve

h = interval width

and y_i = absorbance of fraction i

The integration is applied in two parts, first using h = 1 from fractions 0 through 10, and then with h = 5 from fractions 10 through 30. Using an estimate of variance for the absorbance readings at 220 nm (see Appendix D), the standard deviation of the calculated areas is obtained as follows;

$$Var(A) = (dA/dy)^2 Var(y) \text{ where A= Simpson rule formula} \qquad (3.3)$$

Therefore for each part of the integration we have

$$Var(A) = 1/3(1 + 4x5 + 2x4 + 1)^2 \times 1.11 \times 10^{-5} \qquad (3.3a)$$

$$= 1.11 \times 10^{-3} \quad \therefore \text{ standard deviation} = \pm 0.0333 \text{ for fractions 0 through 10}$$

and $$Var(A) = 5/3(1 + 4 + 2 + 4 + 1)^2 \times 1.11 \times 10^{-5} \qquad (3.3b)$$

$$= 4.44 \times 10^{-3} \quad \therefore \text{ standard deviation} = \pm 0.0666 \text{ for fractions 10 through 30}$$

This results in the standard deviation for total area calculated being approximately ± 0.1, with the values for area ranging from 0.5 to 10.0.

3.7 Packed Columns: Preparation and Characterization

3.7.1 Glass Bead Preparation

Spherical pyrex glass beads of either 1000, 470 or 285 μm diameter were soaked in Chromerge, chromic acid cleaning solution, overnight and then rinsed thoroughly with distilled water. The beads were then dried overnight in a forced air oven (50°C). Siliconized beads were prepared by treating washed, dried glass beads (470 μm only) with a solution of 10% Surfasil (Pierce Chemical Co. Rockford Illinois) in hexane, followed by washing in distilled water and drying overnight in the oven at 50°C.

3.7.2 Column Dimensions and Packing Material

Glass columns having typical dimensions of 2 cm diameter and 30 cm height were mounted vertically. The exit (bottom) was fitted with flexible tubing which could be clamped to control flow. 7 ml of buffer was added and approximately 10 to 20 glass beads (1000 μm diameter) were put in to form a small plug at the bottom (smaller beads would flow through). The packing beads (dry) were then slowly poured with a funnel into the column until the liquid and bead levels coincided. The column was then tapped to settle the packing and more beads were added. This sequence was continued until the buffer volume was completely packed. The weight of beads added was monitored to ensure uniformity in each column.

3.7.3 Surface Area

Using the derivations of Blumenson (54), the surface area for the column is calculated as a function of void volume and radius of packing material. Packing the dry beads into a known buffer volume allows for a simple calculation of the surface area which does not depend on estimating the void fraction. The total surface area is calculated as follows:

$$S_A = \frac{L}{2r} * \frac{(V/L)}{0.22r^2} * 4r^2 \qquad (3.4)$$

$$= V/0.11r \qquad (3.4a)$$

$$\therefore S_A = 7\ cm^3/0.11 \times ((470 \times 10^{-6})/2\ cm)$$

$$= 270{,}793\ cm^2 \text{ for typical column dimensions} \qquad (3.4b)$$

where L= packing height (cm)

V= void volume (cm^3)

and r= particle radius (cm)

3.8 Experimental Protocol for Red Cell/Packed Column Experiments

The experimental arrangement is shown in Figure 3.4. Typically, 30 ml of a red blood cell suspension was percolated through the packed column, while the required liquid head[a] was maintained . A syringe stoppered onto the top of the column, as shown in Figure 3.4, was used to maintain the liquid head level until the bulk suspension had passed through the packing. Samples of the red cell suspension, both

a. Elaborated in section 4.1.2b

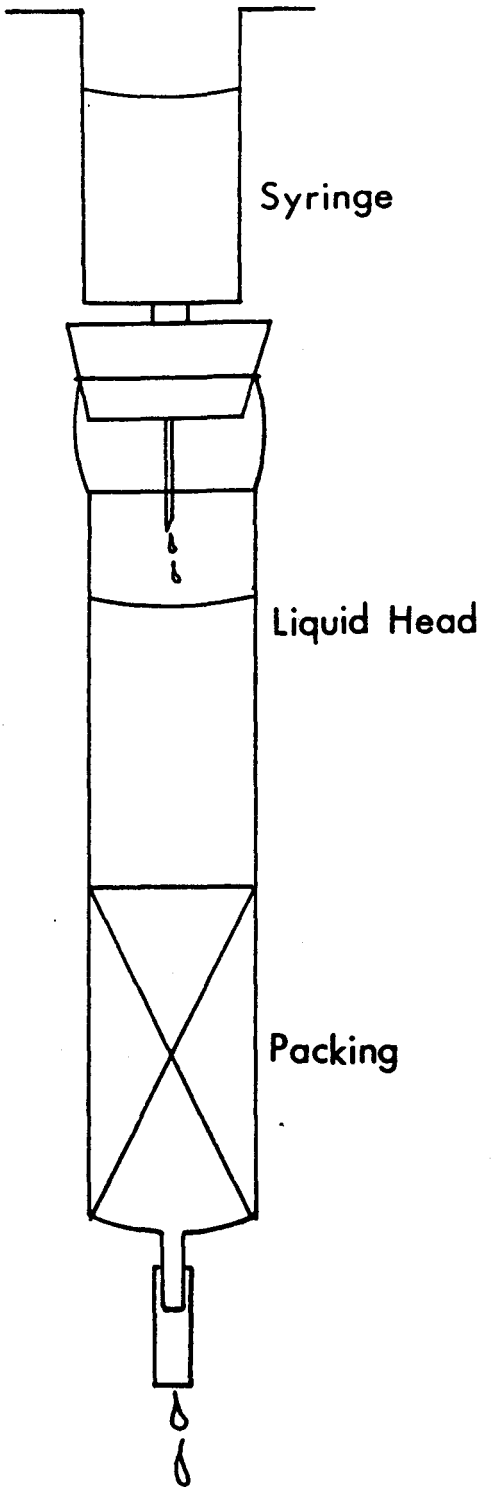

Figure 3.4 Column Configuration; stoppered syringe maintains liquid head

before and after passage through the column, were taken and centrifuged (1000 x g, 10 minutes) to obtain supernatant samples. The hemoglobin assay was performed on these supernatant samples. Without allowing the column to run dry, it was washed first with 125 ml PBS (including the buffer required to maintain the liquid head), followed by 75 ml of distilled water. A solution of 2 % SDS in PBS was then applied to the column, and using a fraction collector 30 fractions of approximately 2 ml each were collected at a rate of approximately one fraction per minute. Finally, the absorbance of each fraction both at 220 and 280 nm was determined and areas calculated for the resulting chromatograms. Control experiments consisted of running 12, 18, and 24 ml samples of suspension supernatants through the column, to correspond to 60, 40, and 20% hematocrit red cell suspensions respectively. Data obtained from the control columns provide baseline values for the "experimental" chromatograms. The result, y, for each column run is calculated as:

$$y = \frac{\text{area of chromatogram for experiment column}}{\text{area of chromatogram for control column}}$$

The use of a ratio normalizes the results from each experiment to a common denominator, since the adsorption of "extracellular" material must be recognized. As well the ratio can be considered as the fraction of surface area covered by red cell deposit relative to any other adsorption that occurs in the absence of the red cells. This acknowledges the fact that material present in the supernatants of the cell suspensions does adhere to the packed column surface.

The experimental protocol described above was used to produce the data required for the experimental design, described in the following section, 3.9. In addition variations on the typical protocol were performed. For example, larger columns (void volume = 10 cm^3, 30 ml load of cell suspension) were run to produce samples for SDS-PAGE analysis, since eluates collected from the smaller columns were too dilute to load on the gels even when concentrated 10-fold. Concentrating the samples further also concentrated the SDS content which in turn tended to clog the ultrafiltration membrane.

In order to obtain the bead samples for either SEM analysis or in the case of the ^{99m}Tc labelled cells, gamma counting, the elution steps were omitted and the beads removed from the columns by suction. For SEM analysis, the beads were immediately placed in a 2% glutaraldehyde solution.

The last variations involved altering the PBS used to resuspend the washed red cells. First, columns were run to investigate the effect of "incubating" the cells in PBS. Although since the experiments were completed within one hour of collecting the blood this was not considered a problem. To check the condition of the cells, parallel experiments were performed using PBS or PBS with 1g/l glucose as the suspending medium. In these runs samples of the cells were taken both before and after passage through the column and examined microscopically. Secondly, EGTA or EDTA was added to PBS to determine the effect of chelating divalent cations. With these columns the original protocol of loading, washing, eluting, as well as

the chromatographic analysis was followed, with the exception that the "control" column was taken as the red cell suspension in PBS alone.

3.9 Experimental Design

A fractional three-level factorial design was chosen to compare and evaluate the effects of hematocrit, shear rate and presence of plasma proteins on the quantity of red cell membrane material deposited on the column packing. Since this study is investigating a virtually unknown phenomenon, a general screening approach, such as with a factorial design, is a logical plan of action. Using the fractional factorial design developed by Box and Behnken (55), 3 variables can be tested in 15 experimental runs. It is desirable to keep the number of experiments low, to avoid having to use more blood donors than necessary. The design matrix used to define the experiments is given in Table 3.3. Scaling the factors to +1 (high), -1 (low) and 0 (center), allows for greater numerical accuracy (56) as well as ease of calculation. Scaling also ensures that the results will not be influenced by choice of units. The equations used to scale the factors are given in Table 3.4.

Table 3.3 Experimental Design Matrix

Experiment#	Factor x_1 Hematocrit	Factor x_2 Shear Rate	Factor x_3 Plasma Content
1	+1	+1	0
2	-1	-1	0
3	+1	-1	0
4	-1	+1	0
5	+1	0	+1
6	-1	0	-1
7	+1	0	-1
8	-1	0	+1
9	0	+1	+1
10	0	-1	-1
11	0	+1	-1
12	0	-1	+1
13	0	0	0
14	0	0	0
15	0	0	0

Table 3.4 Scaling Equations

Factor	Code
Hematocrit (%), HCT	$x_1 = (HCT-40)/20$
Surface Shear Rate, SSR	$x_2 = (-SSR^2+38*SSR-480)/300$
% Plasma, PP	$x_3 = (PP-50)/50$

A second order polynomial, equation 3.5, can readily be fitted to the data generated from the design matrix by using linear least squares analysis.The equations used to obtain the coefficients are listed below (equations 3.6a to 3.6d).

$$y = b_1x_1 + b_2x_2 + b_3x_3 + b_{11}x_1^2 + b_{22}x_2^2 + b_{33}x_3^2 + b_{12}x_1x_2 + b_{13}x_1x_3 + b_{23}x_2x_3 + b_0 \quad (3.5)$$

$$b_o = y_o = \text{mean of center points} \quad (3.6a)$$

$$b_i = 1/8(iy) \quad (3.6b)$$

$$b_{ii} = 3/16(iiy) - 1/16 \sum (jjy) - y_o/2^a \quad (3.6c)$$

$$b_{ij} = 1/4(ijy) \quad (3.6d)$$

where:

$$(iy) = \sum_{u=1}^{N} x_{iu}y_u \quad (3.7a)$$

$$(iiy) = \sum_{u=1}^{N} x_{iu}^2y_u \qquad (jjy) = \sum_{u=1}^{N} x_{ju}^2y_u \quad (3.7b)$$

$$(ijy) = \sum_{u=1}^{N} x_{iu}x_{ju}y_u \quad (3.7c)$$

and N = number of experimental runs

The purpose of fitting a mathematical model to the data, is to create a way of testing the significance of the design variables. It should be emphasized that derived model is not intended to represent a functional form of the phenomenon, and is only useful in determining the relative importance of the factors studied.

a. e.g. $b_{11} = 3/16(11y) - 1/16(22y + 33y) - y_o/2$

Owing to the orthogonal properties of the experimental design, the significance of the coefficients can be tested independantly[a] using an analysis of variance, i.e. F-test (56). Equation 3.8 indicates the the ratio tested against the appropriate F-distribution value at the 95% confidence level. The remaining equations, 3.9a-d, are used to calculate the sum of squares associated with the terms.

$$F = \frac{\text{mean square associated with the term}}{\text{residual mean square}} \qquad (3.8)$$

$$SSb_0 = (y_o)^2/N \quad \text{where N= \# runs} \qquad (3.9a)$$

$$SSb_1 \text{ or } SSb_2 \text{ or } SSb_3 = 1/8(iy)^2 \qquad (3.9b)$$

$$SS(b_{11} + b_{22} + b_{33}) = b_0(y_o) + b_{ii}(iiy) - (y_o)^2/N \qquad (3.9c)$$

$$SSb_{12} \text{ or } SSb_{13} \text{ or } SSb_{23} = 1/4(ijy)^2 \qquad (3.9d)$$

where SSb_i or SSb_{ij} is the sum of squares associated with the b_i or b_{ij} coefficient

In summary, the 3^3 fractional factorial design allows for a convenient and statistically sound analysis of the three experimental variables of interest.

a. However the quadratic coefficients b_{11}, b_{22}, and b_{33} are slightly correlated with each other and are thus grouped together for the F-test (56)

RESULTS AND DISCUSSION

4.1 Packed Column - Establishing Experimental Protocol; Preliminary Experiments

4.1.1 Packing Material; Selecting Bead Size

Pyrex glass beads having average diameters of 1000, 470 and 285 μm were used to test ascertain the best bead size for use with a packed column arrangement. Clearly a balance must be struck between maximizing surface to volume ratio (minimizing bead diameter) while maintaining the biological stability of the red cells. The extent of cell damage leading to hemolysis was determined from the hemoglobin content of the supernatant. Typical values of the change in supernatant hemoglobin concentration after passage of a 40% hematocrit suspension (in PBS) through the column for different size beads are listed in Table 4.1. As can be seen hemolysis increases with decreasing

Table 4.1 Increase in Hemoglobin Content of Supernatant After Passage of Cells Through Column[a]

Bead Size (μm)	Increase in Hemoglobin Concentration (mg/ml ± S.D)[b]	Number of Experiments
1000	0.10 ± 0.02	4
470	0.12 ± 0.05	7
285	>>2[c]	3

a. bed dimensions and red cell load were the same for all columns

b. Pre-column supernatant concentration was 0.13 ± 0.05 mg/ml (n=7)

c. Hemoglobin concentration was beyond range of the calibration curve (2 mg/ml)

particle diameter, and is relatively small in the case of 470 and 1000 μm beads. Based on these results 470 μm beads were used for subsequent experiments. Using a liquid volume of 7 ml of buffer to pack the columns as described in Chapter 3, the red cell suspensions are exposed to approximately 270,800 cm^2 of bead surface, as calculated using equations 3.4 and 3.4a

4.1.2 Flow Rates and Shear Rates

a) Power Law Rheological Model For RBC Suspensions

To describe the flow of red cell suspensions in the packed column, a rheological model was required. Owing to the fact that blood is a particulate fluid, it exhibits non-Newtonian behavior at low shear rates. The Casson equation,

$$\sqrt{\tau} = \sqrt{\tau_y} + \sqrt{\eta\dot{\gamma}} \qquad (4.1)$$

where τ = local shear stress
τ_y = yield stress
η = viscosity coefficient
and $\dot{\gamma}$ = shear rate

best describes whole blood behaviour (57). However for red cell suspensions, the power law model,

$$\tau = k\dot{\gamma}^n \qquad (4.2)$$

where:
$\dot{\gamma}$ = shear rate
τ = shear stress
and k and n=power law constants

is sufficient (57). For this study the data of Brooks et al (58) was used to calculate the power law constants k and n for various hematocrits and buffer or plasma suspending media. Taking data represented in the form of η_i versus $\dot{\gamma}_i$ plots, values of τ_i were calculated ($\tau_i = \eta_i \dot{\gamma}_i$ - based on Weissenberg rheogoniometer (59)) at

the hematocrit values reported. Corresponding log τ_i versus log $\dot{\gamma}_i$ data were assembled and linear regressions performed to determine slope (n) and intercept (k) data. The calculated values are tabulated (Table 4.2) below for both plasma and saline. By interpolating the results, constants n and k for 20, 40 and 60% hematocrits were obtained (Table 4.3). To include the case of 50% plasma/50% PBS, arithmetic means are calculated using whole plasma and PBS data.

Table 4.2 Linear Regression Results For Power Law Parameters Based on Data from Brooks et al (58)

	HCT(%)	n	k	correlation coefficient
PBS	18.96	1.00	0.014	1.00
	28.54	0.98	0.023	0.9996
	40.10	0.89	0.57	0.9989
	47.40	0.79	0.100	0.9915
	55.83	0.76	0.184	0.9997
	69.29	0.71	0/292	0.9992
PLASMA	13.13	1.03	0.030	0.9999
	29.90	0.83	0.086	0.9986
	37.40	0.76	0.152	0.9952
	50.00	0.69	0.294	0.9968
	64.35	0.65	0.410	0.9925

Table 4.3 Interpolated n and k Values

	HCT	n	k
PBS	20	1.00	0.015
	40	0.89	0.056
	60	0.73	0.247
PLASMA	20	0.95	0.053
	40	0.74	0.181
	60	0.66	0.375
50/50 PBS/PLASMA	20	0.97	0.034
	40	0.82	0.119
	60	0.69	0.311

b) Column Conditions

To calculate the shear rate at the packing surface, the rheological model for red cell suspensions described above (section 4.2.1a) was used with the equations derived by Christopher and Middleman (60) for power law flow through a packed bed. These equations are:

$$\dot{\gamma}_s = ((3n+1)/4n) \times (12V_o/(150K\epsilon)^{1/2}) \quad (4.3)$$

$$V_o = (K \triangle P/HL)^{1/n} \quad (4.4)$$

$$H = (k/12) \times (9 + 3/n)^n (150K\epsilon)^{(1-n)/2} \quad (4.5)$$

$$Q = \rho V_o;\ V_o = Q/A_x \quad (4.6a,b)$$

$$K = (Dp^2 \epsilon^3)/(150(1-\epsilon)^2) \quad (4.7)$$

$$A_x = V/(\pi D_c^2 L/4) \quad (4.8)$$

where: $\dot{\gamma}_s$ = shear rate (s^{-1})
n,k = power law constants
V_o = superficial velocity in bed (cm/s)
K = bed "permeability" (cm^2)
ϵ = void fraction
V = void volume (cm^3)
L = packing height (cm)

and H = non-newtonian bed factor (dynes-$s^n/cm^{(n+1)}$)
ΔP = pressure drop (dynes/cm^2)
ρ = fluid density (g/cm^3)
Q = mass velocity (g/cm^2s)
A_X= column cross-sectional area (cm^2)
D_p= particle diameter (cm)
D_C= column diameter (cm)

The validity of the equations was tested experimentally as follows

Conditions: L= 11cm + liquid head= 17cm

measured volumetric flow rate Q= 12cm^3/min

V_O= 0.11cm/s using equation 4.6b

(A) using: $\Delta P = \rho\, g(L + 17)$= 29,000 dyne/$cm^2$

calculate: $\dot{\gamma}_s$= 173.33 s^{-1} and V_O= 0.13cm/s using equations 4.2 and 4.3

(B) using: V_O= 0.11 cm/s

calculate: $\dot{\gamma}_s$= 146.97 s-1 and

ΔP = 30,750 dyne/cm2 using equations 4.2 and 4.3

The values for $\dot{\gamma}_s$ are shown to be reasonable by comparing the results with calculations for power law flow in a tube. Thus for a flow rate of 12 ml/min and using

$$\dot{\gamma}_{wall} = \frac{(3n+1)}{4n} * \frac{4\rho V_O}{\pi R^3} \qquad \text{where R = tube radius} \qquad (4.9)$$

for tube flow, $_{wall}$ values are 0.622 and 262.3 s^{-1} for R equal to 0.75 and 0.10 cm respectively.

A trial and error process was used to calculate the required liquid head to give shear rates of 50, 150 and 300 s^{-1}, for 20, 40 and 60% hematocrits in the different suspending media (namely PBS, plasma or 50/50 plasma/PBS). The detailed results are listed in Appendix E, and the relevant values are shown below in Table 4.4.

Table 4.4 Liquid Head Corresponding to Various Shear Rates (values in cm of buffer)

	HCT	50 s^{-1}	150 s^{-1}	300 s^{-1}
PBS	20	-	0	11
	40	0	13	35
	60	11	36	68
PLASMA	20	0	19	46
	40	6	26	52
	60	13	39	68
50/50	20	0	11	32
	40	4	25	52
	60	12	38	70

c) Verification of Red Cell "Biostability"

Normal preparations of red cell suspensions will undergo slight hemolysis resulting in a free hemglobin concentration of approximately 0.1 mg/ml. All red cell suspensions used had supernatant hemoglobin concentrations of 0.13 $\pm$ 0.05 mg/ml (n=7). As well normal biconcave cell shape was maintained both before and after passage through the column as verified by microscopic examination. Red cell shape change and/or fragmentation was not evident in either the normal PBS preparation or in a parallel preparation in which 1g/l glucose was added to the PBS. As shown in Table 4.5, results from a PBS run and a

glucose supplemented PBS run are virtually indentical. This would suggest that "ageing" or ATP losses from incubation in the PBS without glucose are not likely to be the source of any surface (column) deposit.

Table 4.5 Comparison of Column Elution Profiles With and Without Glucose in the Suspending Medium

Fraction #	A_{220} PBS column	A_{220} PBS + 1g/l glucose column
1	0.445	0.432
2	0.322	0.202
3	0.248	0.099
4	0.182	0.104
5	0.133	0.145
6	0.120	0.173
7	0.116	0.155
8	0.108	0.132
9	0.090	0.123
10	0.077	0.112
AREA $\pm$ 0.1 =	1.896	1.717

4.2 Qualitative Analysis of Column Eluates (Red Cell Membrane Material)

4.2.1 UV - Visible Spectroscopy

Obtaining absorption spectra of the column eluates is a relatively quick and simple procedure. Comparison of the column eluate spectra with that of red cell ghosts solubilized in 2% SDS in PBS (eluting buffer) provided the first indication that membrane derived material is deposited on the packing surface. Typical spectra of red cell ghosts, column eluates, hemolysate, and plasma are shown in Figure 4.1. This figure emphasizes the close similarity between the column eluate and red cell membrane, and highlights the differences between eluates and hemolysate or plasma. It should be

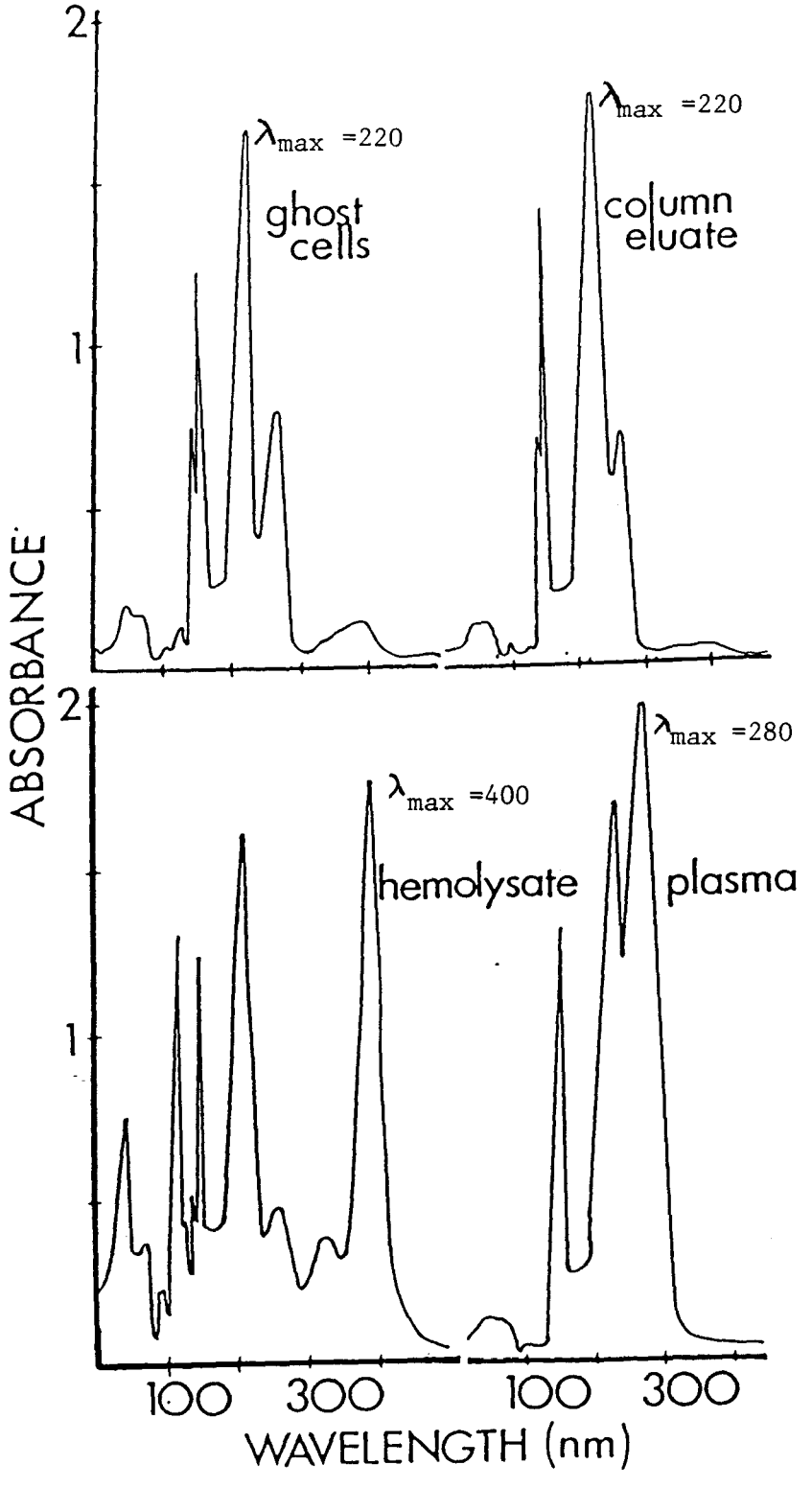

Figure 4.1 UV-Visible Spectra of Various Samples

noted that there is little if any absorbance at 400 nm in the column eluate spectrum. This observation argues against the existence of significant quantities of hemoglobin or intracellular material in the eluate (see hemolysate spectra showing strong absorbance at 400 nm),and also indicates that trapped whole cells are not the material eluted from the columns. Control experiments were performed to check the possibility that the membrane components observed on the packing surface might simply be fragments from cells that were lysed either during suspension preparation or in the hypotonic column washing step. In these control experiments glass bead columns were exposed to hemolysate containing approximately 0.2 mg/ml hemoglobin and a few residual membrane fragments. Under these conditions no membrane material was deposited as only hemoglobin was detected in the column eluates. This suggests that membrane components eluted after exposure to cell suspensions are indeed due to contact with intact red cells.

Data obtained for both raw glass and siliconized glass beads were virtually identical, suggesting a generality for the phenomena with regard to the hydrophilicity or hydophobicity of the surfaces. The "red cell effect" showing inhibition of plasma protein adsorption by red cells, occurred to approximately the same extent on both polyethylene and glass tubing as reported in the publications of Brash and Uniyal (1,2). This is in accordance with the generality of membrane deposition observed in the column experiments.

No conclusion regarding the actual composition of the deposit can be drawn from the UV-visible spectra. However, reviewing the spectra (Figure 4.1), λ_{max} is observed at approximately 220 nm. This information is used to obtain quantitative data, i.e. A_{220}'s (UV absorbance at 220 nm) are obtained for the eluate fractions collected and chromatograms constructed. This analysis is elaborated in the section on quantitative results.

4.2.2 SDS-PAGE - Identification and Proposed Modes of Deposition of Red Cell Membrane Material

Characterization and positive identification of the "deposit" is accomplished using gel electrophoresis. A typical SDS-PAGE result is shown in Figure 4.2. As can be seen there is good correspondence between the protein composition of the column eluates and that of ghost cell membranes, hence the results support and substantiate the UV-visible spectra. Unlike the UV-visible spectral data, good gel results were difficult to obtain using the collected fractions. Conventional Coomassie Blue staining was not sensitive enough even for samples that were concentrated 20-fold by ultrafiltration. Acceptable results were eventually obtained using silver stain which is up to 50-fold more sensitive than Coomaisse Blue (52). It seems that UV-visible spectroscopy is sensitive to both lipid (at 220 nm (53)) and protein (at 280 nm), whereas the SDS-PAGE silver stain identifies only protein. Therefore it is suggested that the relative ease with which spectral data versus gel results were obtained may indicate a

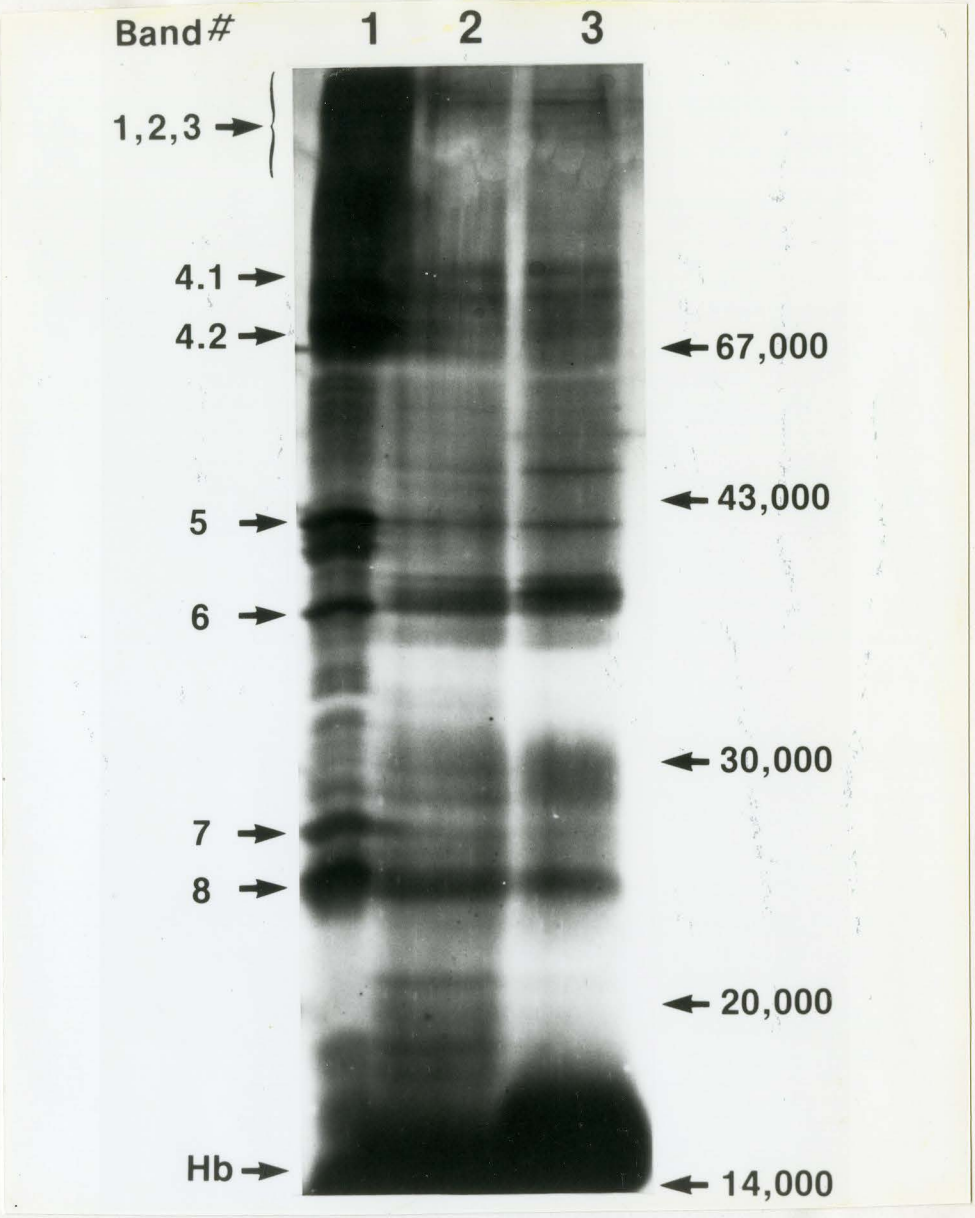

Figure 4.2 SDS-PAGE of Various Samples; key to lanes: 1) ghost cell membrane
2) glass bead column eluate
3) siliconized glass bead column eluate
Numbers on left correspond to naming system of Fairbanks (23). Numbers on right are molecular weight values at corresponding gel positions

higher lipid content relative to the protein content than in red cell membrane. It is interesting to note that in human red cell membrane the weight ratio of lipid to protein is approximately 0.8 (9).

Interpretations regarding composition and mode of deposition of the membrane components are based principally on the analysis of the SDS-PAGE data. The protein composition of the column eluate corresponds to that of the ghost membranes with the notable difference that bands[a] 1, 2 (spectrin) and 7 are not present in the eluate, and band 5 (actin) is relatively weak compared to the whole cell membrane. Since passage through the column does not cause significant hemolysis, it is to be expected that the cytoskeleton of the red cells will remain intact and consequently cytoskeletal components such as spectrin and actin (27) will not be associated with the material deposited on the column surface. The lack of these proteins in the eluate as indicated by the SDS-PAGE data, is in accord with this expectation. The lack of protein may contribute to the apparent high lipid to protein weight ratio mentioned earlier. It is important to point out the possibility that some membrane proteins may adhere so strongly to the bead surface that they are not eluted, although this is not likely since SDS is known to solubilize all the red cell membrane proteins (23).

From the literature and from the SDS-PAGE data obtained in the present work, two mechanisms regarding the mode of red cell membrane

a. Nomenclature of Fairbanks (23)

material deposition may be hypothesized. Firstly, Allen et al (39) describe "microvesicles" that arise from a "budding-off" membrane reaction, when red cells are treated with an ionophore to increase the membrane permeability to Ca^{2+}. The SDS-PAGE data shown by Allan et al (39) indicate that the vesicles are similar to red cell membranes, except that they lack cytoskeletal proteins, bands 1, 2, and 5, and have an increased level of hemoglobin. The composition of these vesicles correlates closely with that of the column eluate, thus suggesting that a comparable mechanism may be occurring in the column experiments described here. Shear and/or deformation of the red cells resulting from flow through the narrow spaces of the column may physically induce the "blebbing-off" (61) of membrane material which subsequently adheres to the surface. The likely variation of red cell membrane pore size versus membrane tension for a brief exposure to stress, without lysis, has been published by Blackshear (62) and is shown in Figure 4.3. This figure illustrates that ions could permeate the membrane, leaking in or out well before hemolysis would occur.

Tether formation is the second proposed mode of membrane component deposition in the column. This situation involves cell adhesion followed by the application of shear forces which cause a red cell "tether" to form. An SEM of red cell tethers was shown earlier in Figure 2.9. Tether formation in the packed columns would likely result from the flow patterns in the narrow interstices of the column rather than from the cells settling and attaching prior to being sheared off as described by Hochmuth (44). Cell-cell interactions

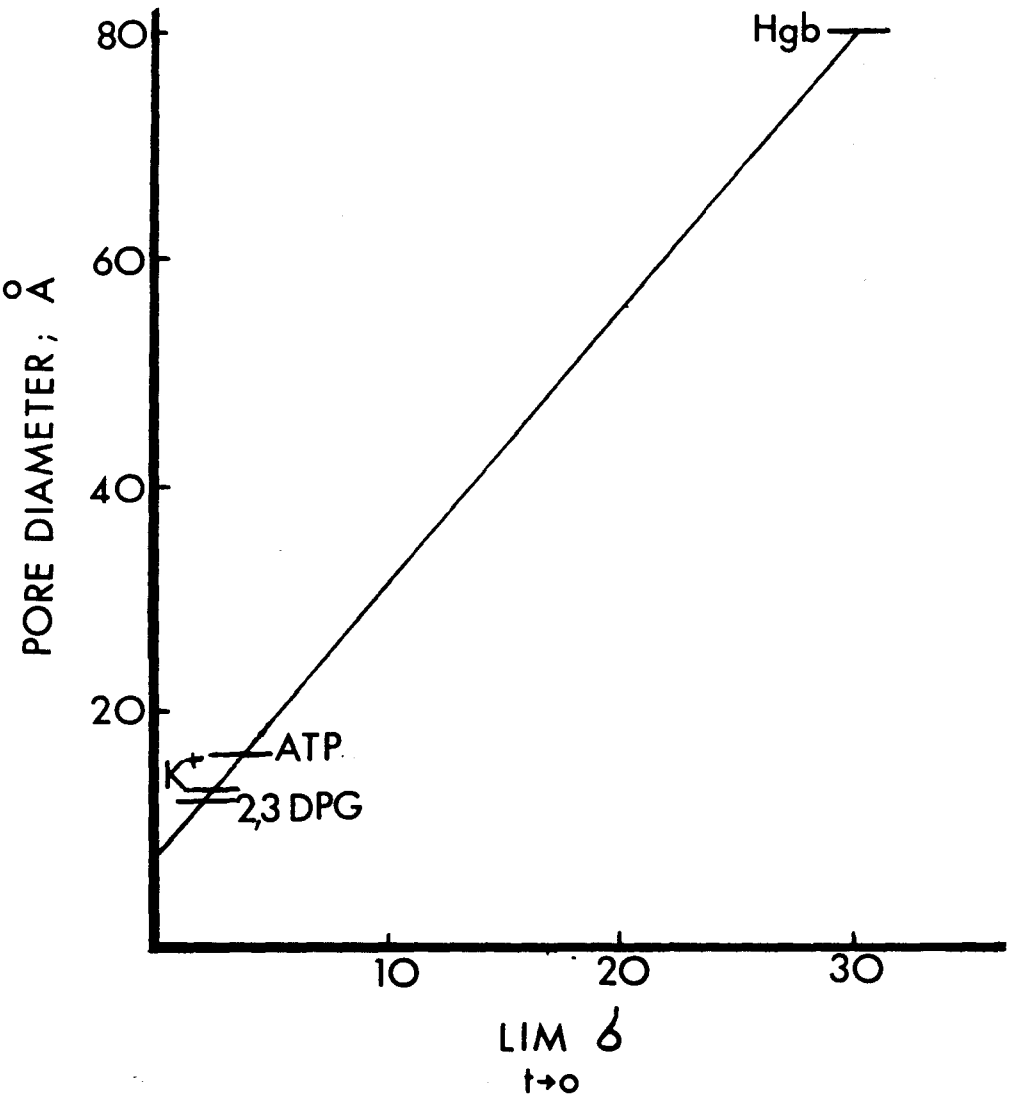

Figure 4.3 Estimate of Membrane Pore Size vs. Membrane Tension (62)

such the cells "squeezing" other cells against the surface as shown by Goldsmith (63) for tube flow, may also contribute to tether formation. More evidence to support these hypotheses was sought using scanning electron microscopy.

4.2.3 Scanning Electron Microscopy

Figures 4.4a-4.4d show typical SEM data for the glass beads after exposure to red cell suspensions. SEM analysis of beads before RBC exposure indicated a clean surface with no detectable "deposits". The proposed mechanisms of both tether and vesicle formation are supported by these micrographs. Figures 4.4b and 4.4c illustrate a tether-like deposit, the dimensions of which correspond to typical tether dimensions as described by Hochmuth (44) and Blackshear (62). As for the vesicle-type deposit as shown in Figure 4.4d, the dimensions of this deposit are in accord with those found by Allen et al (39), for vesicles formed from Ca^{2+} loaded red cells. The presence of the "vesicles" in the vicinity of the tethers has also been reported by Benser et al (41), who also noted that the vesicles arise from lipid segregated from the red cell tethers (41). Scanning electron micrographs shown in Figures 4.5a and 4.5b, represent the bead surface after exposure to red cells resuspended in autologous plasma. These micrographs are less definitive than those seen in Figure 4.4, but they do indicate a filamentous deposit. It should be noted that the tethers and vesicles are in general frequently rather than rarely observed, thus making it unlikely that they represent random cell debris.

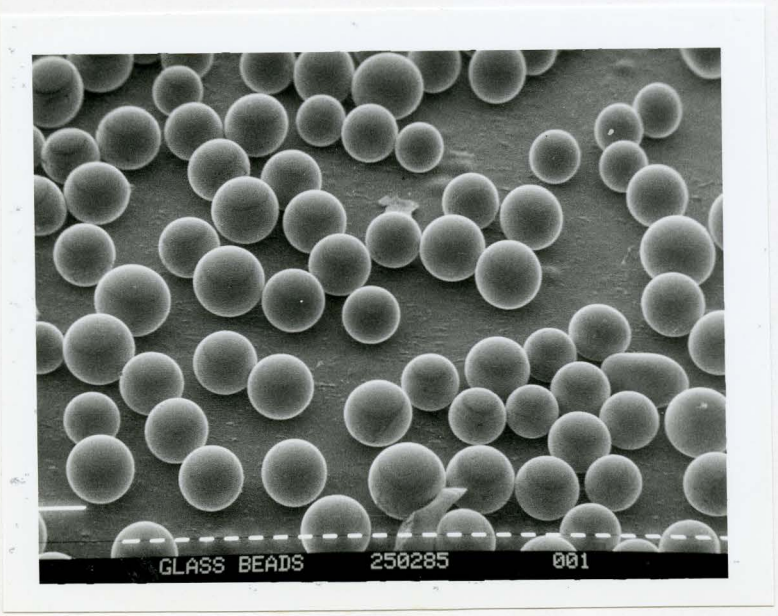

4.4a

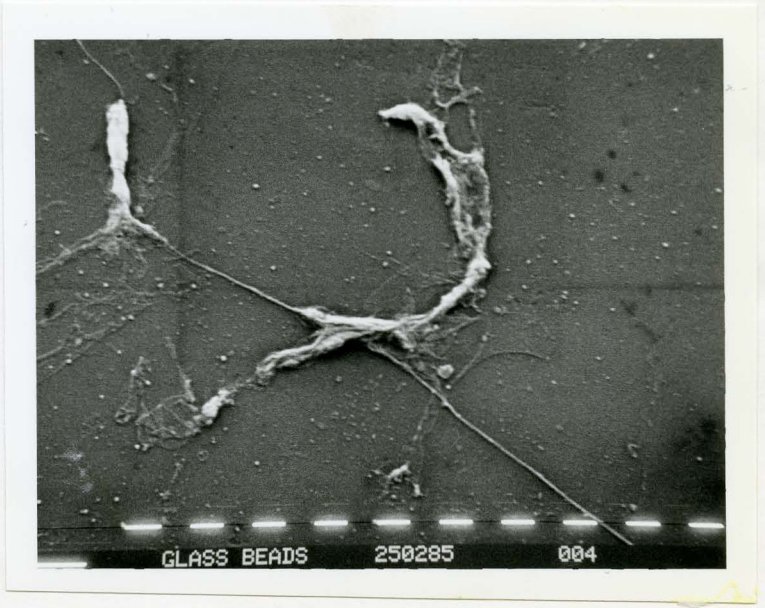

4.4b

Figure 4.4a-d SEM of Glass Beads from PBS Experiments; (a) low magnification 20x, marker = 100 μm, (b) "tether" 5000x, marker = 1 μm, (c) "tether" 20,000x, marker = 1 μm, (d) "vesicles" 85,000x, marker = 1 μm

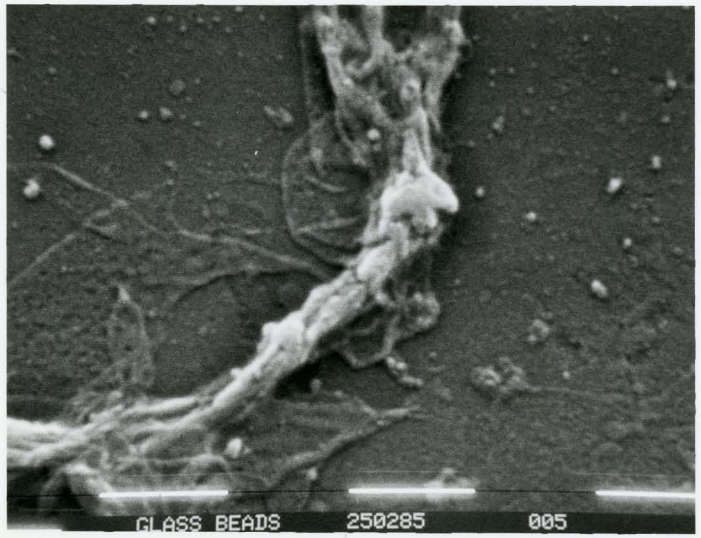

4.4c

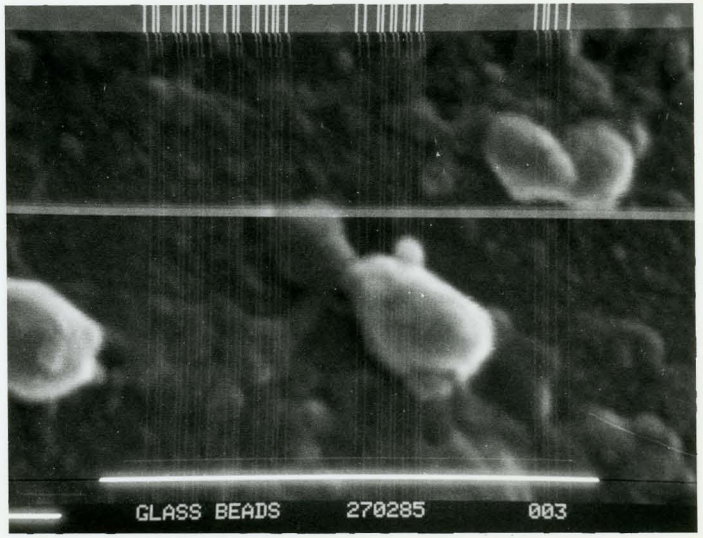

4.4d

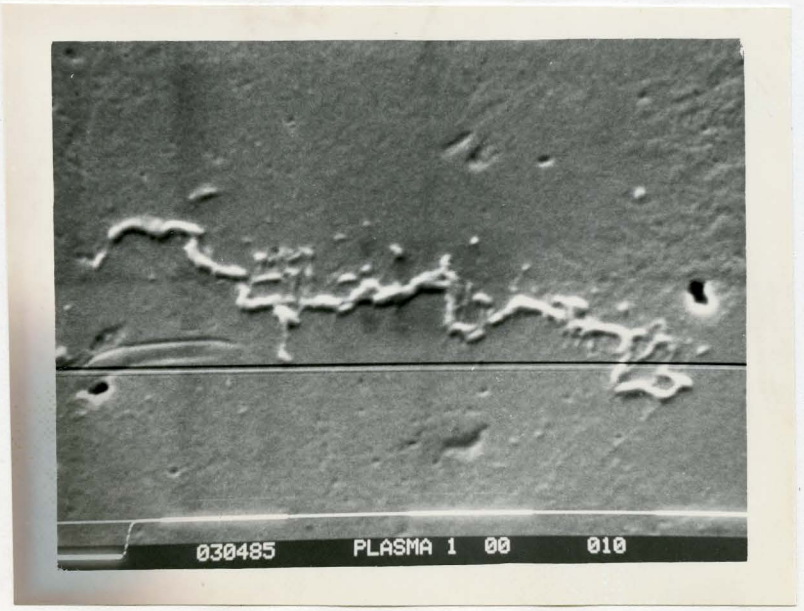

4.5a

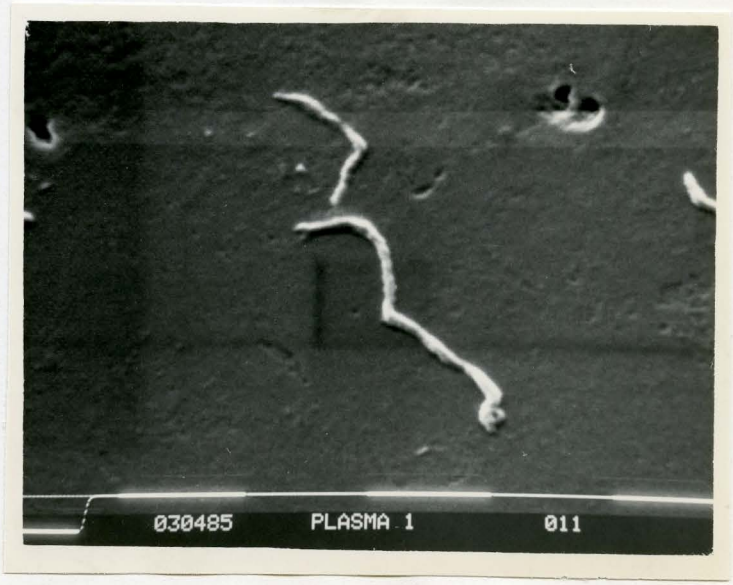

4.5b

Figure 4.5a-b SEM of Glass Beads from Plasma Experiments; (a) and (b) 20,000x, marker = 1 μm

4.2.4 Effect of Divalent Cations on Deposition of Membrane Material

The suggested "blebbing" (61) mechanism for the red cell deposit was investigated by manipulating the environment of the resuspended red cell. Due to their chemical structure, ethylenediametetracetic acid (EDTA) and ethylenebis-(oxy-ethylenenitrilo)tetracetic acid (EGTA) chelate divalent cations, in particular, Mg^{2+} and Ca^{2+}. EGTA has the greater affinity for Ca^{2+}. Either EDTA or EGTA at a concentration of 0.5mM were added to isotonic PBS, to assess the importance of Ca^{2+} on the amount of membrane material deposited in the column experiments. To test an extreme case one column experiment was performed using 5mM EDTA. The results of these experiments are listed in Table 4.6. At 0.5mM concentrations the effects appear to be insignificant. However, at a 5mM EDTA concentration, virtually no material was deposited. These results suggest that the divalent cations may influence the red cell membrane deposition. The cations possibly facilitate cell-bead interactions by providing a bridge between the two negatively charged surfaces.

Table 4.6 EDTA/EGTA Experiment Results

Experiment	Result[a]
EGTA 0.5mM	1.234
EDTA 0.5mM	1.302
EDTA 5.0mM	0.000

a. result = ratio of areas of the A_{220} chromatograms, i.e. column with chelator added to column with no chelator added, ±.1 S.D.

4.3 Quantitative Analysis

The data discussed above established that membrane material is indeed deposited on surfaces in contact with red blood cells, and provided some indication regarding the specific nature of the deposited material. In a second phase of the project it was desirable to develop a method to quantify the effect and to further investigate its phenomenology, i.e. to assess the effect of experimental variables such as the presence of plasma proteins, flow conditions, and hematocrit on the quantity of material deposited in the column experiments.

Quantification of the material in the columns using UV analysis at 220 nm has already been described in this chapter (section 4.2.1). The phenomenological aspects were investigated using the fractional factorial design explained in Chapter 3. Prior to all this, however, radioactive technetium labelled red cells were used in the initial attempts to quantify the deposit.

4.3.1 ^{99m}Tc Labelled Red Cells - Experiments

Concurrent with the qualitative investigations using gel electrophoresis, red cells were labelled with ^{99m}Tc, as described in Chapter 3, in an attempt to quantify the material deposited on the columns. Two assumptions were made regarding the use of the ^{99m}Tc label for quantification experiments before the SDS-PAGE data describing the column elutes were obtained; first it was assumed that the deposited material is representative of the membrane as a whole and is not a selective "extract" of the membrane and second that the

^{99m}Tc label is randomly distributed in the membrane so that it would be representative of the deposited material. From the report of Thompson et al (49), an autoradiograph of an SDS-PAGE of ^{99m}Tc labelled red cells, showed that both hemoglobin (intracellular) and membrane proteins are labelled (see Figure 4.5). Therefore control experiments using hemolysate contaminated supernatant were performed to check for accumulation of radioactivity on the surface due to non-membrane related material (intracellular material labelled with ^{99m}Tc). Typical results are shown in Table 4.7. The fact that some radioactivity does accumulate can most likely be attributed to hemoglobin adsorption. This adsorption is acknowledged but is not of concern since less than 0.1 percent of the total radioactivity applied accumulates in the typical experimental column.

Table 4.7 ^{99m}Tc Experiment Results Deposition of Radioactivity on Glass Beads Under Various Conditions

Suspending Medium	HCT	% Radioactivity on Beads[a]
PBS	40	0.047 0.076 0.075
PBS	0	0.064
Plasma	40	0.003
Plasma	0	0.003
50% Plasma in PBS	40	0.011
Hemolysate 2 mg/ml Hgb	-	0.403

a. based on the total radioactivity of the red cells applied to the column

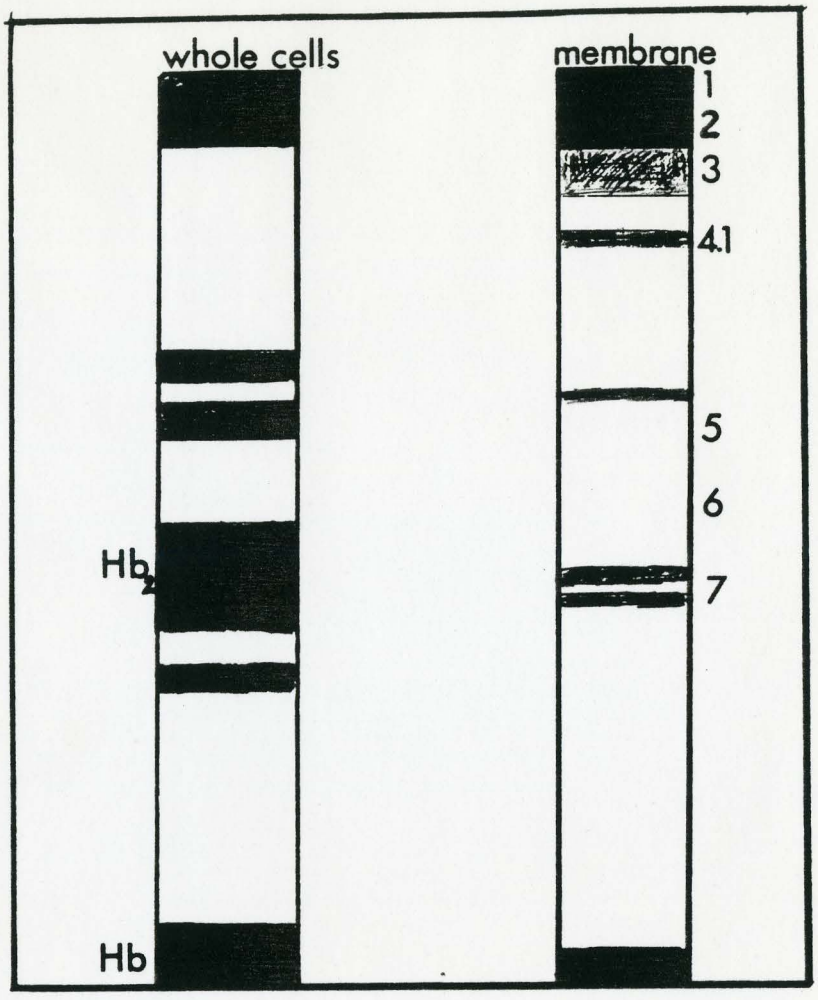

Figure 4.6 Schematic of an 11% SDS-polyacylamide gel autoradiograph of whole red cells and red cell membranes labelled with ^{99m}Tc (49)

It should be emphasized again that the SDS-PAGE results presented earlier (section 4.2.2), were obtained after the bulk of the ^{99m}Tc experiments were completed. In retrospect, comparing the gel autoradiograph of ^{99m}Tc labelled cells (Figure 4.6) with the SDS-PAGE data obtained for column eluates, the results shown in Table 4.7 are easily explained. The radioactive label is concentrated in the integral membrane proteins which are not present in the column eluates. Therefore one would expect very little radioactivity to accumulate in the columns. This is confirmed in Table 4.7.

It was concluded that experiments with technetium labelled red cells could not be used to quantify the membrane material deposited on the beads since the labelled membrane components were not representative of the material eluted from the columns. However, the data collected does provide supporting evidence regarding the specific nature of the deposit.

4.3.2 3^3 Fractional Factorial Design

The experimental conditions of this study are given below in Table 4.8, and are based on the design matrix outlined in Chapter 3. The corresponding experimental results (given as the ratio of A_{220} or A_{280} chromatograph areas, experiment:control) are also listed. It should be pointed out the data provide an indication of the amount of surface deposit and not an absolute measure of the quantity of material deposited.

Typically, five columns were run on a given day. Two were control columns and three were "experimental" columns. The grouping of runs for each day was arranged to optimize the use of the red cells available (approximately 45 ml washed, packed cells per day) and to randomize the order of the experiments as indicated by the second column in Table 4.8.

Table 4.8 Experimental Design Results

Ex#	Day[a]	HCT%	Shear Rate (s^{-1})	% Plasma in suspending medium	y= area exp/area control	
					A_{220}	A_{280}
1	E	60	300	50	1.513	1.541
2	F	20	50	50	0.632	0.530
3	C	60	50	50	1.470	1.485
4	E	20	300	50	0.656	0.668
5	C	60	150	100	1.850	2.269
6	E	20	150	0	0.839	0.764
7	F	60	150	0	1.702	1.522
8	E	20	150	100	0.675	0.805
9	D	40	300	100	1.136	1.308
10	A	40	50	0	1.676	1.960
11	A	40	300	0	1.398	1.463
12	B	40	50	100	1.071	1.346
13	B	40	150	50	1.024	0.758
14	D	40	150	50	1.426	1.600
15	D	40	150	50	1.428	1.708

a. represents daily grouping of runs in random order

Using the procedure of Box and Behnken (55), the polynomial "models" derived from the experimental design results may be expressed as follows;

$$Y_{A220} = 1.294 + 4.665x_1 - 0.018x_2 - 0.110x_3 - 0.139x_1^2 - 0.084x_2^2 + 0.113x_3^2 + 0.005x_1x_2 + 0.078x_1x_3 + 0.086x_2x_3 \quad (4.10)$$

and

$$Y_{A280} = 1.355 + 0.506x_1 - 0.043x_2 + 0.002x_3 - 0.239x_1^2 - 0.060x_2^2 + 0.224x_3^2 - 0.204x_1x_2 + 0.177x_1x_3 + 0.115x_2x_3 \quad (4.11)$$

where x_1 = scaled hematocrit, x_2 = scaled shear rate, x_3 = scaled plasma concentration, and $Y_{A220/A280}$ = result at either 220 or 280 nm

The significance of the coefficients is determined as discussed in Chapter 3 using F-tests in the manner suggested by Bacon (56). The results are summarized for both models in Tables 4.9a and 4.9b. Based on this statistical analysis, the conclusion is drawn that of the three variables studied, only hematocrit (i.e. only those coefficients related to x_1) has a significant effect on the amount of membrane related material deposited on the column. Graphical representations of the data (A_{220} results), shown in Figures 4.7a-c confirm the results of the F-test analysis. As can be seen, there is a positive and relatively good correlation between membrane material deposited and hematocrit and no apparent correlation with either shear rate or % plasma concentration. Furthermore the A_{280} analysis supports these conclusions with similar results (Table 4.9b).

Table 4.9a F-Test Summary, y_{A220} Data

Sum of Squares due to terms	d.f.	mean square assoc with each term	F=m.s. assoc with term /residual m.s[a].
b_0 22.807	1	22.807	511.604[b]
b_1 1.741	1	1.741	39.053[b]
b_2 0.003	1	0.003	0.058
b_3 0.097	1	0.097	2.180
b_{11} b_{22} 4.138 b_{33}	3	1.379	30.942[b]
b_{12} 0.000	1	0.000	0.000
b_{13} 0.024	1	0.024	0.547
b_{23} 0.030	1	0.030	0.662

a. residual mean square = 0.2128
b. denotes coefficients significantly different from zero tested against F = 6.608 (1d.f. 95% confidence) or F = 5.40951 (3 d.f. 95%).

Table 4.9b F-Test Summary, y_{A280} Data

Sum of Squares due to terms	d.f.	mean square assoc with each term	F=m.s. assoc with term /residual m.s[a].
b_0 25.939	1	25.939	121.898[b]
b_1 2.050	1	2.050	9.653[b]
b_2 0.015	1	0.015	0.068
b_3 0.000	1	0.000	0.000
b_{11} b_{22} 5.228 b_{33}	3	1.743	8.189[b]
b_{12} 0.002	1	0.002	0.008
b_{13} 0.125	1	0.125	0.585
b_{23} 0.053	1	0.053	0.247

a. residual mean square = 0.2128
b. denotes coefficients significantly different from zero tested against F = 6.608 (1d.f. 95% confidence) or F = 5.40951 (3 d.f. 95%).

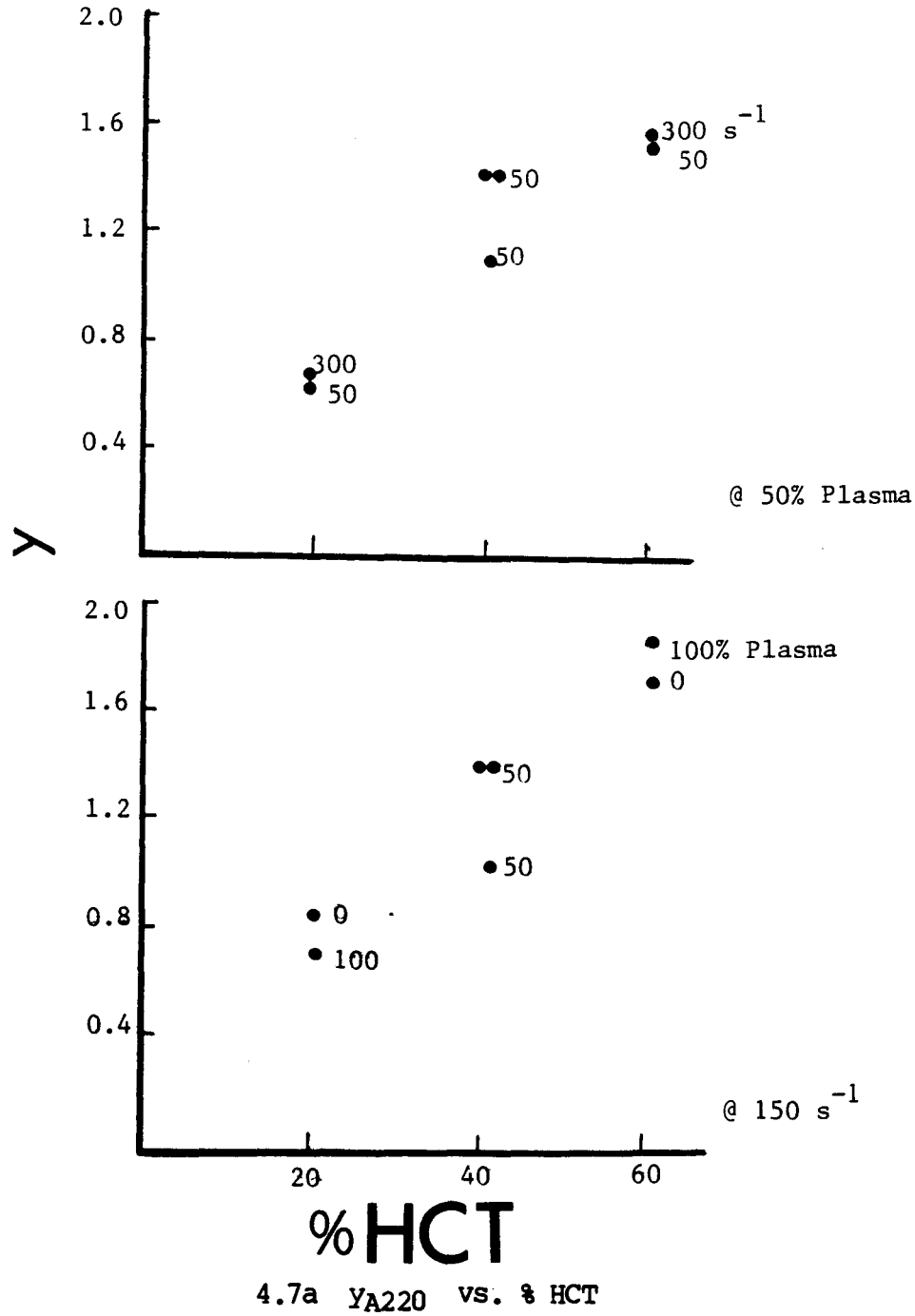

4.7a Y_{A220} vs. % HCT

Figure 4.7a-c Graphical Representation of Experimental Design Data

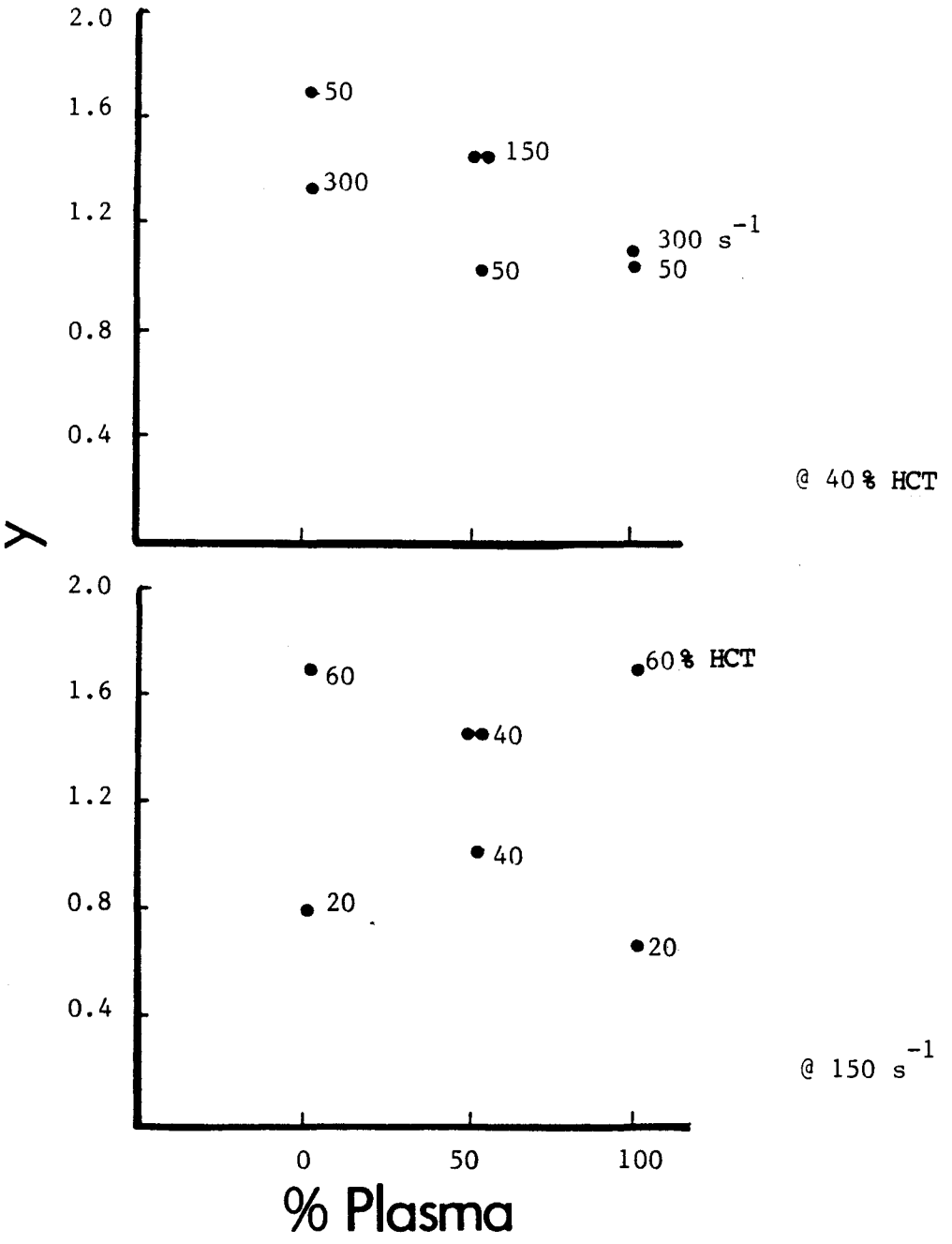

4.7b y_{A220} vs. % plasma

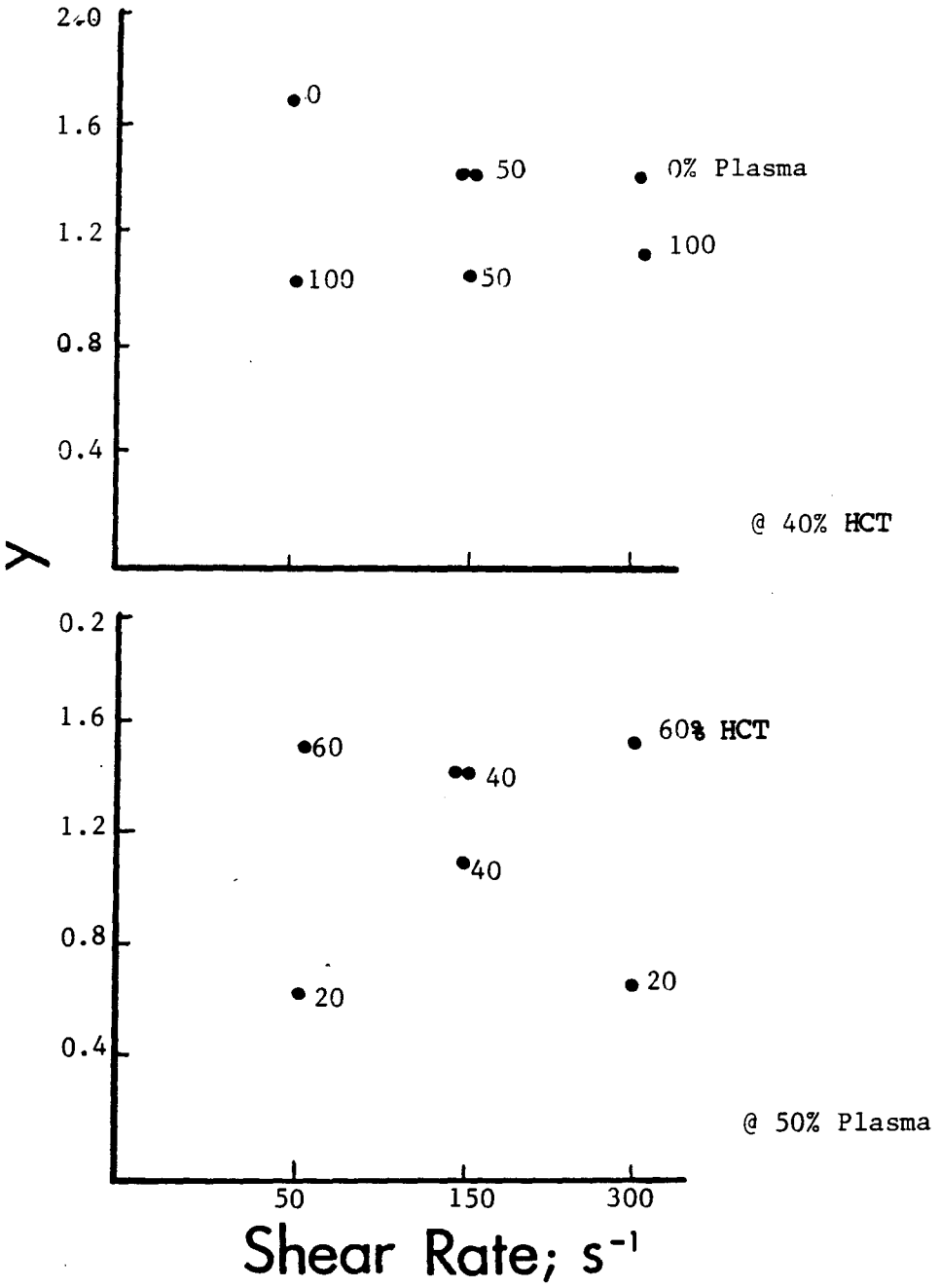

4.7c Y_{A220} vs. Shear Rate

There are however limitations involved with his experimental design, which must be recognized and considered before excluding the effects of shear rate and plasma content on membrane material deposition. These are:

(1) the fractional factorial design can be described as a "one shot" type of experimental design (56), which attempts to gather as much information as possible from a limited number of experimental runs. The smaller the pool of blood donors required, however, the less variability in the red cell source. Dual A_{220} and A_{280} analysis compensates to some extent for the small experimental data base since they provide concurring results.

(2) The estimates of average shear rates in the column could be misleading. The distribution of shear rates may be broad. Certainly, the flow patterns and shear rate in the column are not well defined compared to say simple tube flow. Also the range chosen, 50 s^{-1} to 300 s^{-1}, may have been too narrow, although this range was dictated by practical limits. It was desirable to avoid pumping the red cell suspensions, as this could only complicate the investigation by introducing mechanical trauma and foreign surface contact, ie tubing contact, prior to contacting the glass bead surface.

(3) Both SEM and data obtained using ^{99m}Tc labelled red cells illustrate differences between PBS and plasma experiments. Therefore the presence of plasma may be complicating the

phenomenon to a greater degree than is revealed by UV analysis of the eluates, and directly comparing experiments which involved PBS with those using plasma could be beyond the capabilities of the UV-chromatographic analysis.

Combining the results from the experimental design, with the evidence accumulated from UV-visible spectroscopy, SDS-PAGE, SEM, and ^{99m}Tc experiments, the red cell deposit phenomenon has been indentified and preliminary characterization data on the deposited material has been obtained.

SUMMARY AND CONCLUSIONS

This investigation of red blood cell-foreign surface contact provide evidence to confirm the hypothesis that cell membrane derived components are deposited onto contacting surfaces. SDS-PAGE data provides the most conclusive evidence and reveal the protein composition of the deposit. The material consists of the peripheral and some integral red cell membrane proteins, with the noted exception of the major cytoskeletal components, spectrin and actin. It is also speculated that the deposit contains a high lipid to protein weight ratio. The phenomenon is visualized as a tether-like mode of deposition, and/or the result of membrane vesiculations. SEM photographs substantiate these findings.

Investigation of the effect of experimental conditions, in particular hematocrit, surface shear rate and the presence of plasma in the suspending medium, showed a positive correlation between hematocrit and amount of material deposited. However no definite conclusions could be drawn regarding shear rate and plasma content.

Despite the fact that red cells are the most abundant single constituent of human blood, their potential role relating to the adverse reaction of blood to "biomaterials" has been largely overlooked. This neglect probably stems from the fact that red cells are generally not considered to have a direct role in thrombus formation. Red cells are however, known to increase platelet adhesion to surfaces (13), and platelet retention in packed columns (64).

A "red cell effect" has also been describe, by which plasma protein adsorption to glass and polyethylene is inhibited in the presence of red cells (1,2). Wolfe et al (65), feel that the failure to devise a satisfactory artificial blood compatible interface, is a reflection of our ignorance of many basic factors involved in cell-surface contact. Undoubtedly red cells should be considered in this context. The red cell membrane material found to be deposited on the glass bead packing in the present work, is essentially a product of cell-surface contact, perhaps involving transient adhesion.

To relate these observations to the "bio-incompatability" of foreign surfaces with blood, one must discuss their relationship to thrombus formation. The protein and the lipid content of the red cell deposit, has definite potential to affect coagulation, as certain phospholipids provide an amphipathic environment which can act as a catalytic interface for clotting factors (30). On the other hand this membrane related material may be causing the "red cell effect", by covering surface sites which would otherwise adsorb plasma proteins. Obviously there is no simple answer, but this study does prove that red cells can contribute to blood-surface interactions in manners not yet explored.

The more that is known, the more complex biomaterials research becomes. Apart from the conventional approach to study blood elements and coagulation , it has also been suggested that researchers look beyond blood clotting as the sole index of biocompatability, for example to the complement system (65). It seems entirely logical that

the body's self defense mechanisms operate in conjunction with hemostasis and thrombosis of foreign surfaces. Recently, Davies and Cohen (18) reported that platelets appear to contain proteins that are immunologically related to red cell membrane proteins. Perhaps some answers can be found by studying these immunological links between red cell and platelet membranes in the context of foreign surface induced thrombosis.

In summary, the contribution of the present study is that a red cell membrane derived deposit on a contacting foreign surface was identified and a preliminary description of the phenomenon involved was accomplished. It is hoped that this work will promote greater respect for the red cell as an important factor in blood biomaterials interactions, and will prompt continued work on Uniyal's (1) and other potential "red cell effects".

REFERENCES

1. Uniyal, S., Brash, J.L., Degterev, I.A., Adv. Chem. Series, 199, 277 (1982)

2. Brash, J.L., Uniyal, S., Trans. Amer. Soc. Artif. Int. Organs, 22, 253 (1976)

3. Peppas, N.A., AC.S., 199, 465 (1982)

4. Chawla, A.S., Sipehia R., J.Biomed. Mater. Res., 18, 537 (1984)

5. Schmitt, J.M., Baer, M., Meindl, J.D., Anderson, M.F., Mihm, F.G., J.Biomed. Mater. Res., 18, 797 (1984)

6. Baier, R.E., Ann. N.Y. Acad. Sci., 283, 17 (1977)

7. VanDulm, P., Norde, W., J.Coll. Int. Sci., 91, 248 (1983)

8. Horbett, T.A., Adv. Chem. Series, 199, 233 (1982)

9. Surgenor, D.M., editor, The Red Blood Cell, volumes I and II, Academic Press, N.Y. (1974)

10. Robertson, C.R., Chang, H.N., Ann. Biomed. Eng., 2, 361 (1974)

11. Turitto, V.T., Weiss, H.J., Ann. N.Y. Acad. Sci., 416, 363 (1983)

12. Vroman, L., Adams, A.L., Fischer, G.C., Munoz, P.G., Stanford, M., Adv. Chem. Series, 199, 265 (1982)

13. Brash, J.L., Brophy, J.M., Feurestein, I.A., J.Biomed. Mater. Res., 10, 429 (1976)

14. Keller, K.H., Yum, S.I., Trans. Amer. Soc. Artif. Int. Organs, 16, 42 (1970)

15. Winters, S., Gendreau, R.M., Leininger, R.I., Jakobsen, R.J., Appl. Spectr., 36, 404 (1982)

16. Hirsh J., Brain E.A., Hemostasis and Thrombosis a Conceptual Approach, 2nd edition, Churchill Livingston Publication, (1983)

17. Hoffman, A.S., Adv. Chem. Series, 199, 3 (1982)

18. Davies, G.E., Cohen, C.M., Blood, 65, 52 (1985)

19. Bruck, S.D., Ann. N.Y. Acad. Sci., 283, 352 (1977)

20. ------, Dorland's Pocket Medical Dictionary, 23rd edition, W.B. Saunders Company, (1982)

21. Singer, S.J., Nicolson, G.L., Science, 175, 720 (1972)

22. Cohen, C.M., Sem. Hematol., 20, 141 (1983)

23. Fairbanks, G., Steck, T., Wallach, D.F.H., Biochem., 10, 2606 (1971)

24. Steck, T.L., J. Cell Biol., 62, 1 (1974)

25. Anderson, N.L., Anderson, N.G., Proc. Natl. Acad. Sci., 74, 5421 (1977)

26. Morrison, M., Mueller, T.J., Edwards, H.H., Prog. Clin. Biol. Res., 55, 17 (1981)

27. Mueller, T.J., Morrisom, M., Prog. Clin. Biol. Res., 56, 95 (1981)

28. Marchesi, V.T., Prog. Clin. Biol. Res., 159, 1 (1984)

29. Schwartz, R.S., Chui, B.T., Lubin, B., Prog. Clin. Biol. Res., 159, 89 (1984)

30. Zwall, R.F.A., Biochim. Biophys. Acta, 515, 163 (1978)

31. Lubin, B., Chui, D., Roelofsen, B., VanDeenen, L.L.M., Prog. Clin. Biol. Res., 56, 171 (1981)

32. Mohandas, N., Chasis, J.A., Shohet, B., Sem. Hem., 20, 225 (1983)

33. Eaton, J.W., Prog. Clin. Biol. Res., 56, 1 (1981)

34. Mehta, N.G., Biochim. Biophys. Acta, 762, 9 (1983)

35. Evans, E.A., Hochmuth, R.M., Biophys. J., 16, 1 (1976)

36. Lacelle, P.L., Evans, E.A., Hochmuth, R.M., Blood Cells, 3, 335 (1977)

37. Indeglia, R.A., Bernstein, E.F., Trans. Amer. Soc. Artif. Inter. Organs, 16, 37 (1970)

38. Mohandas, N., Clark, M.R., Feo, C., Jacobs, M.S., Shohet, S.B., Prog. Clin. Biol. Res., 55, 423 (1981)

39. Allan, D., Billah, M.M., Finean, J.B., Michell, R.H., Nature, 261, 58 (1976)

40. Allan, D., Thomas, P., Limbrick, A.R., Biochem. J., 188, 881 (1980)

41. Benser, A., Meyer, H.W., Linss, W., Geyer, G., Acta Histochem. Suppl., 23, 263 (1981)

42. Evans, E.A., Hochmuth, R.M., Biophys. J., 16, 13 (1976)

43. Sutera, S.P., Mehrjard, M.H., Biophys. J., 15, 1 (1975)

44. Hochmuth, R.M., Mohandas, N., Spaeth, E.E., Williamson, J.R., Blackshear, P.L.Jr., Johnson, D.W., Trans. Amer. Soc. Artif. Inter. Organs, 18, 325 (1972)

45. Hochmuth, R.M., Mohandas, N., Blackshear, P.L.Jr., Biophys. J., 13, 747 (1973)

46. Steck, T.L., in Methods in Membrane Biology, Plenum Press N.Y., 2, 245 (1974)

47. Burton, G.W., Ingold, K.U., Thompson, K.E., Lipids, 16, 946 (1981)

48. Sigma Diagnostics, Technical Bulletin No. 525, Sigma Chemical Company St. Louis, Missouri, (revised 1982)

49. Thompson, S., Newman, P., Maddy, A.H., Br. J. Hem., 49, 575 (1981)

50. Biorad, Price List J. Chromatography, Electrophoresis, Immunochemistry, HPLC, Biorad Laboratories, Richmond California, (January 1984)

51. Laemmli, U.K., Nature, 227, 680 (1970)

52. Biorad Silver Stain, Bulletin No. 1089, Biorad Laboratories, Richmond California, (1982)

53. Long, M.M., Urry, D.W., in Molecular Biology Biochemistry and Biophysics, No. 31 Membrane Spectroscopy, Springer Verlag Publ., (1981)

54. Blumenson, L.E., J. Cell Physiol., 70, 23 (1967)

55. Box, G.E.P., Behnken, D.W., Technometrics, 2, 455 (1960)

56. Bacon, D.W., Ind. Eng. Chem., 62, 27 (1970)

57. Whitmore, R.L., in Rheology of the Circulation, Oxford Pergammon Press, (1968)

58. Brooks, D.E., Goodwin, J.W., Seaman, G.V.F., J. Appl. Phys., 28, 172 (1970)

59. Dealy, J.M., in Rheometers for Molten Plastics, Van Nostrand Rheinhold Corp., (1982)

60. Christopher, R.H. Middleman, S., Ind. Eng. Chem. Fund., 4, 422 (1969)

61. Hope, M.J., Cullis, P.R., FEBS Letters, 107, 322 (1979)

62. Blackshear, P.J.Jr., Fed. Proc., 30, 1709 (1971)

63. Goldsmith, H.L., Fed. Proc., 30, 1578 (1971)

64. Hopen, G., Scand. J. Haem., 22, 226 (1979)

65. Wolf, H., Gringell, D., J. Cell Sci., 63, 101 (1983)

66. Lindsay, R.M., Manson, R.G., Kim, S.W., Andrade, J.D., Hakim, R.M., Trans. Amer. Soc. Artif. Inter. Organs, 26, 603 (1980)

APPENDIX A

(i) Red Cell Suspensions; The recipes are based on the assumption of 15% buffer by volume in the packed red cells. Therefore,

desired hematocrit x total volume required =

volume of packed red cells ÷ 1.15

Recipe values are then adjusted by taking hematocrit readings of suspensions (using microhematocrit tubes and a microcentrifuge), to give the proportions outlined in Chapter 3.

(ii) Phosphate Buffered Saline (PBS)

3.63g KH_2PO_4 + 15.15g Na_2HPO_4 + 10.55g NaCl

make to 2.0 litres, pH 7.35 This solution is isotonic

APPENDIX B

Hemoglobin Assay Modification; This method is based on the Sigma protocol (44) for determining the hemoglobin content in whole blood. The original protocol was adjusted for a 200-fold increase in sensitivity to accommodate the low concentration of hemoglobin in the experimental samples.

Original protocol: S = sample volume 0.020 ml

D = drabkins reagent 5.000 ml

T = total volume 5.020 ml

S/T = 1/251, and S/T must be < 1, therefore S can be increased up to 251 times the original volume. A 200-fold increase was chosen , and S taken as 2 ml for convenience.

∴ S/T = 200/251, with S = 2, T = 2.510 ml

consequently D = 0.510 ml

Modified protocol: S = 2.000 ml

D = 0.510 ml

and T = 2.510 ml

APPENDIX C Gel Electrophoresis Information

(i) SDS PAGE Buffers and Reagents; Laemmli procedure (51)

reagents:

1. 30% acryl-0.8% Bis : 30.0 g acrylamide + 0.8 g methylenebis acrylamide made to 100 ml and refrigerated.

2. 10% ammonium persulfate initiator, $(NH_4)_2S_2O_8$: 1 g ammonium persulfate + 10 ml distilled H_2O made fresh each time.

3. 20% SDS in H_2O : 100 g SDS made to 500 ml

4. 10% by weight glycerol in H_2O : 5 g glycerol made to 50 ml and refrigerated

5. 0.5% N,N,N',N'-tetramethylethylenediamine (TEMED), catalyst in H_2O : 5 ml 5% TEMED made to 50 ml and refrigerated.

6. Separating Gel Buffer, 1.5M Tris/HCl : 181.7 g Tris made to 1 litre, pH adjusted to 8.8 with concentrated HCl.

7. Stacking Gel Buffer, 0.5M Tris/HCl : 30.3 g Tris made to 500 ml, pH adjusted to 6.8 with concentrated HCl.

8. Tracking Dye, 1% bromophenol blue in H_2O : 0.5 g bromophenol blue made to 50 ml

9. Reservoir Buffer, 0.25M Tris/1.92M Glycine : 60.0 g Tris + 288.2 g Glycine made to 2 litres.

recipes and protocols

1. Separating Gel : prepare glass plates and make up 11% separating gel as follows;

(a) 18.84 ml H_2O + 15.00 ml Separating Buffer + 21.96 ml 30% acryl-0.8 Bis + 300 µl 20% SDS + 600 µl 10% glycerol, MIX AND DEGAS

(b) ADD JUST BEFORE POURING SLAB, 3.0 ml 0.5% TEMED + 450 µl 10% ammonium persulfate

(c) Polymerize overnight with a slight overlay of distilled water to prevent edge drying

2. Stacking Gel : remove water overlay on separating gel and pour 5% stacking gel prepared as follows;

(a) 7.28 ml H_2O + 3.75 ml Stacking Buffer + 2.85 ml 30% acryl-0.8% Bis + 75 µl 20% SDS + 75 µl 10% glycerol, MIX AND DEGAS

(b) ADD JUST BEFORE POURING, 1.5ml 0.5% TEMED + 450 µl 10% ammonium persulfate

(c) Place combs to form wells for sample loading, and allow to polymerize minimum 2 hours

meanwhile 3. Prepare the electrolyte buffer for the system reservoirs as follows;
800 ml reservoir buffer + 40 ml 20% SDS made to 4000 ml

and 4. Prepare the reducing sample buffer as follows:

2.4 g glycerol + 2.5 ml stacking buffer + 3.0 ml 20% SDS + 1.0 ml 2 β-mercaptoethanol (reducing reagent) + 1.0 ml 1% bromophenol blue

next 5. Select protein samples to be studied, combine approximately 100 µl sample with 100 µl reducing sample buffer (total 200 µl); heat samples at 70° C for 30 minutes, before loading onto gel

finally 6. Set up system and current, allowing 15 to 24 hours for electrophoresis; remove gel and following the staining protocol

(ii) Silver Stain (Biorad (52))

reagents:

1. Oxidizer : 20 ml concentrate + 180 ml H_2O

2. Silver Reagent : 20 ml concentrate + 180 ml H_2O

3. Developer
4. Fixatives : A-40% methanol/10% acetic acid (v/v)
B-10% ethanol/5% acetic acid (v/v)

5. Stop : 5% acetic acid (v/v)

protocol: place gel in tray with reagents as follows;

i) Fixative A, 400 ml, 60 min
ii) Fixative B, 400 ml, 30 min
iii) Fixative B, 400 ml, 30 min
iv) Oxidizer, 200 ml, 10 min
v) Deionized Water, 400 ml, 20 min
vi) Deionized Water, 400 ml, 20 min
vii) Deionized Water, 400 ml, 20 min
viii) Silver Reagent, 200 ml, 30 min
ix) Deionized Water, 400 ml, 2 min
x) Developer, 200 ml, 1 min
xi) Developer, 200 ml, approx. 5 min
xii) Developer, (if necessary), 200 ml, 5 min
xiii) Stop, 400 ml, 5 min

APPENDIX D A_{220} Miscellaneous Information

(i) Variance of Absorbance at 220 nm Readings 20 random readings at A_{220} of a representative sample were taken

1. 0.166	11. 0.175
2. 0.172	12. 0.177
3. 0.173	13. 0.175
4. 0.170	14. 0.173
5. 0.172	15. 0.177
6. 0.183	16. 0.176
7. 0.174	17. 0.172
8. 0.181	18. 0.175
9. 0.176	19. 0.174
10. 0.174	20. 0.173

mean = 0.1745, std.dev. = 0.0034105, var. = 0.0000111

(ii) Standard Deviation of Calculated y Values;

y = area of experiment chromatograph/area of control = AE/AC

$$\mathrm{Var}(y) = (dy/dAE)^2\mathrm{Var}(AE) + (dy/dAC)^2\mathrm{Var}(AC)$$

$$\therefore \quad \mathrm{Var}(y)/y^2 = \mathrm{Var}(AE)/AE^2 + \mathrm{Var}(AC)/AC^2$$

and std. dev. $(y) = \mathrm{Var}(y)^{1/2}$

two sample calculations show:

ex# 1	AE = 6.6840	AC = 4.4187	y = 1.5127	and std dev. =	0.04
2	5.7995	8.8375	0.6562		0.01

APPENDIX E

$\dot{\gamma}_s$ Trial and Error Calculations;

Conditions: $\epsilon = 0.36$
$\rho = 1.07$ g/cm^3
$g = 981$ cm/s^2
$D_p = 0.047$ cm
$h_p = 11$ cm
$D_C = 1.5$ cm
Vol.= 7 ml

ΔP = (dynes/cm^2)
Q = (g/cm^{2}s)
V_o= (cm/s)
$\dot{\gamma}_s$= (s^{-1})

	h_L =	1 cm	5	10	17	0	11	
20% HCT	P	12,596	16,795	22,043	29,391	11,546	23,093	
PBS	Q	0.2293	0.3060	o.4018	0.5360	0.2112	0.4210	
	V_o	0.1298	0.1731	0.2274	0.3033	0.1189	0.2382	
	$\dot{\gamma}_s$	163.71	218.41	286.82	382.65	150.04	300.51	
						35	0	13
40% HCT	P	12,596	16,795	22,043	29,391	48,285	11,546	25,192
PBS	Q	0.0920	0.1270	0.1722	0.2376	0.4143	0.0835	0.2000
	V_o	0.0521	0.0719	0.0974	0.1345	0.2345	0.0472	0.1132
	$\dot{\gamma}_s$	67.62	93.32	126.54	174.63	304.48	61.34	146.95
						11	36	68
60% HCT	P	12,596	16,975	22,043	29,391	23,093	49,334	82,924
PBS	Q	0.0291	0.0432	0.0627	0.0929	0.0378	0.1887	0.3842
	V_o	0.0165	0.0244	0.0355	0.0526	0.0378	0.1068	0.2174
	$\dot{\gamma}_s$	22.70	33.65	48.83	72.39	52.04	147.07	299.37
						0	19	46
20% HCT	P	12,596	16,975	22,043	29,391	11,546	31,490	59,831
Plasma	Q	0.0794	0.1076	0.1435	0.1956	0.0724	0.2093	0.4129
	V_o	0.0449	0.0609	0.0812	0.1101	0.0410	0.1185	0.2337
	$\dot{\gamma}_s$	57.45	77.90	103.89	140.86	52.40	151.53	298.91
						6	26	52
40% HCT	P	12,596	16,975	22,043	29,391	17,844	38,838	66,129
Plasma	Q	0.0420	0.0619	0.0891	0.1312	0.0671	0.1910	0.3897
	V_o	0.0238	0.0350	0.0504	0.0742	0.0380	0.1079	0.2205
	$\dot{\gamma}_s$	32.56	47.92	69.04	101.60	51.98	147.73	301.91

	h_L =	1 cm	5	10	17	13	39	68
60% HCT	P	12,596	16,795	22,043	29,391	25,192	52,484	82,924
Plasma	Q	0.0212	0.0327	0.0495	0.0766	0.0606	0.1850	0.3707
	V_o	0.0120	0.0185	0.0280	0.0434	0.0343	0.1047	0.2098
	$\dot{\gamma}_s$	17.05	26.40	39.91	61.79	48.88	149.14	298.88
						0	11	32
20% HCT	P	12,596	16,975	22,043	29,391	11,546	23,093	45,136
50% PBS	Q	0.1130	0.1518	0.2010	0.2702	0.1033	0.2108	0.4203
	V_o	0.0639	0.0860	0.1137	0.1529	0.0584	0.1193	0.2378
	$\dot{\gamma}_s$	81.81	109.16	144.43	194.21	74.23	151.52	302.05
						4	25	52
40% HCT	P	12,596	16,975	22,043	29,391	15,745	37,788	66,129
50% PBS	Q	0.0529	0.0751	0.1047	0.1488	0.0694	0.2022	0.4005
	V_o	0.0299	0.0425	0.0592	0.0842	0.0393	0.1144	0.2266
	$\dot{\gamma}_s$	39.80	56.55	78 83	112.01	52.26	152.25	301.56
						24	39	69
60% HTC	P	12,596	16,975	22,043	29,391	24,142	52,484	85,023
50% PBS	Q	0.0243	0.0367	0.0543	0.0822	0.0619	0.1895	0.3797
	V_o	0.0137	0.0208	0.0307	0.0465	0.0351	0.1072	0.2148
	$\dot{\gamma}_s$	19.22	29.08	43.03	65.12	49.05	150.10	300.70

APPENDIX F

Experimental Design Raw Data

(i) Control column data; areas for the control columns were determined on an average basis, i.e. for all runs of 12, 18, and 24 ml calculate the average area per ml for each buffer.

buffer	A_{220} area/ml	A_{280} area/ml
Plasma	0.386	0.050
PBS	0.320	0.040
50% Plasma	0.368	0.053

(ii) Raw data A_{220}'s and A_{280}'s of daily experiments;

15/1/85		ex.10		ex.11		16/1/85 ex.12	
		220	280	220	280	220	280
fraction#	1	0.232	0.035	0.035	0.017	0.000	0.000
	2	0.970	0.230	0.850	0.146	0.330	0.030
	3	0.400	0.059	0.307	0.048	0.160	0.019
	4	0.370	0.057	0.255	0.043	0.155	0.019
	5	0.280	0.050	0.228	0.040	0.190	0.026
	6	0.266	0.048	0.200	0.037	0.212	0.030
	7	0.260	0.050	0.198	0.034	0.222	0.031
	8	0.253	0.047	0.195	0.035	0.239	0.030
	9	0.247	0.046	0.193	0.034	0.253	0.030
	10	0.253	0.050	0.187	0.030	0.227	0.029
	15	0.229	0.041	0.196	0.030	0.198	0.031
	20	0.220	0.040	0.190	0.030	0.182	0.029
	25	0.177	0.032	0.167	0.028	0.170	0.028
	30	0.197	0.035	0.184	0.030	0.193	0.032
area =		9.411	1.734	7.851	1.295	7.440	1.191

16/1/85		ex.13		17/1/85 ex.3		ex.5	
		220	280	220	280	220	280
fraction#	1	0.000	0.000	0.005	0.000	0.004	0.000
	2	0.310	0.024	0.464	0.050	0.620	0.134
	3	0.194	0.016	0.199	0.021	0.341	0.057
	4	0.214	0.023	0.197	0.029	0.315	0.047
	5	0.208	0.023	0.234	0.034	0.290	0.043
	6	0.199	0.025	0.258	0.038	0.270	0.040
	7	0.189	0.020	0.187	0.028	0.247	0.036
	8	0.190	0.023	0.173	0.025	0.228	0.035
	9	0.200	0.024	0.170	0.028	0.219	0.033
	10	0.162	0.017	0.167	0.027	0.206	0.032
	15	0.163	0.017	0.153	0.022	0.205	0.031
	20	0.148	0.017	0.162	0.024	0.218	0.034
	25	0.198	0.021	0.152	0.023	0.185	0.028
	30	0.126	0.014	0.150	0.024	0.230	0.037
area =		6.777	0.722	6.496	0.949	8.572	1.339

21/1/85		ex.14		ex.15		ex.9	
		220	280	220	280	220	280
fraction#	1	0.002	0.000	0.000	0.000	0.081	0.002
	2	0.389	0.046	0.459	0.050	0.430	0.048
	3	0.324	0.049	0.253	0.034	0.275	0.034
	4	0.306	0.048	0.227	0.032	0.336	0.047
	5	0.308	0.049	0.228	0.034	0.454	0.071
	6	0.296	0.046	0.223	0.036	0.233	0.033
	7	0.298	0.051	0.214	0.013	0.208	0.028
	8	0.287	0.048	0.217	0.032	0.194	0.027
	9	0.283	0.045	0.219	0.033	0.193	0.028
	10	0.282	0.046	0.216	0.032	0.199	0.029
	15	0.196	0.034	0.239	0.038	0.175	0.026
	20	0.226	0.042	0.241	0.040	0.161	0.024
	25	0.253	0.046	0.249	0.044	0.179	0.028
	30	0.220	0.041	0.313	0.054	0.231	0.038
area =		9.462	1.627	9.449	1.522	7.896	1.158

22/1/85		ex.1		ex.4		ex.6	
		220	280	220	280	220	280
fraction#	1	0.030	0.016	0.032	0.000	0.083	0.008
	2	0.334	0.037	0.588	0.080	0.334	0.037
	3	0.158	0.019	0.234	0.038	0.133	0.016
	4	0.164	0.020	0.192	0.030	0.148	0.019
	5	0.170	0.023	0.178	0.026	0.155	0.020
	6	0.172	0.024	0.167	0.024	0.150	0.020
	7	0.165	0.022	0.166	0.025	0.152	0.020
	8	0.161	0.024	0.427	0.072	0.150	0.019
	9	0.170	0.028	0.167	0.029	0.149	0.021
	10	0.168	0.026	0.165	0.024	0.145	0.020
	15	0.169	0.024	0.122	0.018	0.146	0.012
	20	0.159	0.024	0.120	0.017	0.181	0.030
	25	0.174	0.026	0.122	0.017	0.169	0.025
	30	0.202	0.031	0.136	0.019	0.161	0.023
area =		6.684	0.985	5.800	0.845	6.286	0.901

22/1/85		ex.8		23/1/85 ex.7		ex.2	
		220	280	220	280	220	280
fraction#	1	0.061	0.000	0.000	0.000	0.000	0.000
	2	0.334	0.037	0.629	0.080	0.337	0.037
	3	0.133	0.016	0.276	0.036	0.154	0.016
	4	0.148	0.019	0.205	0.027	0.182	0.020
	5	0.155	0.020	0.175	0.023	0.216	0.024
	6	0.150	0.020	0.168	0.022	0.227	0.026
	7	0.152	0.020	0.158	0.021	0.220	0.026
	8	0.150	0.019	0.158	0.021	0.208	0.026
	9	0.149	0.021	0.152	0.020	0.169	0.020
	10	0.145	0.020	0.149	0.021	0.145	0.018
	15	0.146	0.021	0.158	0.023	0.121	0.014
	20	0.181	0.030	0.154	0.021	0.128	0.017
	25	0.169	0.025	0.149	0.022	0.143	0.018
	30	0.161	0.023	0.129	0.020	0.100	0.012
area =		6.256	0.950	6.373	0.898	5.589	0.673